SC-M-67-2933
February 1968

AERO-THERMODYNAMICS

A DETAILED DEVELOPMENT OF THE TRICYCLIC THEORY

Harold R. Vaughn, 9321

SANDIA LABORATORIES

OPERATED FOR THE UNITED STATES ATOMIC ENERGY COMMISSION BY SANDIA CORPORATION | ALBUQUERQUE, NEW MEXICO; LIVERMORE, CALIFORNIA

Issued by Sandia Corporation
a prime contractor to the
United States Atomic Energy Commission

LEGAL NOTICE

This report was prepared as an account of Government-sponsored work. Neither the United States, nor the Commission, nor any person acting on behalf of the Commission:

A. Makes any warranty or representation, expressed or implied, with respect to the accuracy, completeness, or usefulness of the information contained in this report, or that the use of any information, apparatus, method, or process disclosed in this report may not infringe privately owned rights; or

B. Assumes any liabilities with respect to the use of, or for damages resulting from the use of any information, apparatus, method, or process disclosed in this report.

As used in the above, "person acting on behalf of the Commission" includes any employee or contractor of the Commission, or employee of such contractor, to the extent that such employee or contractor of the Commission, or employee of such contractor prepares, disseminates, or provides access to, any information pursuant to his employment or contract with the Commission, or his employment with such contractor.

SC-M-67-2933

A DETAILED DEVELOPMENT OF THE TRICYCLIC THEORY

Harold R. Vaughn, 9321
Sandia Laboratory, Albuquerque

February 1968

Second Printing, January 1969

ABSTRACT

A detailed, step-by-step development of the Tricyclic Flight Dynamics Theory originally derived by Dr. John Nicolaides is presented. Examples of application of the theory are included.

CONTENTS

	Page
SUMMARY	5
SYMBOLS	6
Introduction	9
Aeroballistic Equations of Motion	9
Tricyclic Solution to Aeroballistic Equations	19
Application	36
Simplified Equations	36
Example Problem	37
Tricyclic Case	39
Epicyclic Case	40
Discussion	41
Constant Coefficient Restriction	41
Small Angle Restriction	44
Physical Interpretation	44
Characteristic Motion	49
Magnus Moment	51
Conclusions	53
REFERENCES	55
APPENDIX A -- Sample Calculations	57

ILLUSTRATIONS

Figure		
1.	Inertial Axis System	11
2.	Axis System	14
3.	Aeroballistic System	18
4.	Complex Plane	22
5.	Comparison of Tricyclic Theory with 6 DOF Calculation	42
6.	Comparison of Epicyclic Theory with 6 DOF Calculation	43
7.	Effect of Large Angle on $\bar{\alpha}$ and $\bar{\beta}$	45
8.	Physical Interpretation of Tricyclic Theory	46
9.	$\tilde{\alpha}$ - $\tilde{\beta}$ Plot	48
10.	Characteristic Motion with Zero Roll Rate	50
11.	Characteristic Motion of Rolling Body	52

SUMMARY

The Tricyclic Theory was first derived in 1953 by Dr. John D. Nicolaides,[1,2] and has been republished in different forms and extended by others.[3] The Tricyclic Theory is a powerful flight dynamics tool; however, it is by necessity complicated and difficult to understand in detail. The use of complex variables in the theory makes it particularly difficult to interpret on a physical basis. In attempting to apply the theory the author has rederived it for his own use and added some detail that is normally not presented in a formal document. This approach may help other ballisticians and flight dynamicists reach a more complete understanding of the theory.

SYMBOLS

A	- Imaginary ($\bar{\alpha}$) component of K, rad
B	- Real ($\bar{\beta}$) component of K, rad
$C_{n\beta}$	- Yaw moment coefficient due to β, per rad
$C_{m\alpha}$	- Pitch moment coefficient due to α, per rad
$C_{n\dot{\beta}}$	- Yaw moment coefficient due to rate of change of β, $\left[\frac{\partial C_n}{\partial\left(\frac{\dot{\beta}d}{2V}\right)}\right]$ per rad
$C_{m\dot{\alpha}}$	- Pitch moment coefficient due to rate of change of α, $\left[\frac{\partial C_m}{\partial\left(\frac{\dot{\alpha}d}{2V}\right)}\right]$ per rad
C_{nr}	- Yaw moment coefficient due to r, $\left[\frac{\partial C_n}{\partial\left(\frac{rd}{2V}\right)}\right]$ per rad
C_{mq}	- Pitch moment coefficient due to q, $\left[\frac{\partial C_m}{\partial\left(\frac{qd}{2V}\right)}\right]$ per rad
$C_{np\alpha}$	- Magnus moment coefficient due to α, $\left[\frac{\partial C_n}{\partial\alpha\left(\frac{pd}{2V}\right)}\right]$ per (rad)^2
$C_{mp\beta}$	- Magnus moment coefficient due to β, $\left[\frac{\partial C_m}{\partial\beta\left(\frac{pd}{2V}\right)}\right]$ per (rad)^2
d	- Body diameter, feet
H	- Angular momentum
$\vec{i}, \vec{j}, \vec{k}$	- Unit vectors
I_x	- Roll moment of inertia about body x axis (also I_{xx}), slug-ft^2
I_y	- Moment of inertia about body y axis (also I_{yy}), slug-ft^2
I_z	- Moment of inertia about body z axis (also I_{zz}), slug-ft^2
I	- Lateral moment of inertia when $I_y = I_z$, slug-ft^2
I_{xy}, I_{xz}, I_{yx} I_{yz}, I_{zx}, I_{zy}	- Products of inertia, slug-ft^2
K_1	- Nutation arm, rad
K_2	- Precession arm, rad
K_3	- Trim arm, rad
L	- Roll moment, ft-lb
M	- Pitch moment, ft-lb
N	- Yaw moment, ft-lb

SYMBOLS (cont)

M_x, M_y, M_z - Total moments about x, y, and z axes, ft-lb

M_δ - Moment due to control deflection δ, ft-lb/rad

$M_{p\beta}$ - Magnus moment due to β, (Equation 46), $\frac{\text{ft-lb}}{\text{rad}^2/\text{sec}}$

$N_{p\alpha}$ - Magnus moment due to α (Equation 47), $\frac{\text{ft-lb}}{\text{rad}^2/\text{sec}}$

M_α - Pitch moment due to α (Equation 48), $\frac{\text{ft-lb}}{\text{rad}}$

N_β - Yaw moment due to β (Equation 49), $\frac{\text{ft-lb}}{\text{rad}}$

M_q - Pitch moment due to q (Equation 50), $\frac{\text{ft-lb}}{\text{rad/sec}}$

N_r - Yaw moment due to r (Equation 51), $\frac{\text{ft-lb}}{\text{rad/sec}}$

$M_{\dot{\alpha}}$ - Pitch moment due to $\dot{\alpha}$ (Equation 52), $\frac{\text{ft-lb}}{\text{rad/sec}}$

$N_{\dot{\beta}}$ - Yaw moment due to $\dot{\beta}$ (Equation 53), $\frac{\text{ft-lb}}{\text{rad/sec}}$

N_1, N_2, N_3 - Constants in differential equation

$m_{1,2}$ - Two roots of differential equation

p - Roll angular velocity, rad/sec

q - Pitch angular velocity, rad/sec

r - Yaw angular velocity, rad/sec

q' - Dynamic pressure, psf

$\vec{r}$ - Vector distance from origin of axis to elemental mass, ft

S - Body cross sectional area, ft^2

s - Gyroscopic stability factor

t - Time, sec

$\vec{v}$ - Vector velocity of elementary particle m, ft/sec

V - Total free stream velocity, ft/sec

SYMBOLS (cont)

x	- Body roll axis
$\bar{x}$	- Aeroballistic body roll axis
y	- Body pitch axis
$\bar{y}$	- Aeroballistic body pitch axis
z	- Body yaw axis
$\bar{z}$	- Aeroballistic body yaw axis
X, Y, Z	- Inertial reference axis system

GREEK SYMBOLS

α	- Body fixed axis angle of attack
$\bar{\alpha}$	- Aeroballistic angle of attack
$\tilde{\alpha}$	- Aeroballistic angle of attack in 6 DOF axis system
β	- Body fixed axis angle of sideslip
$\bar{\beta}$	- Aeroballistic angle of sideslip
$\tilde{\beta}$	- Aeroballistic angle of sideslip in 6 DOF axis system
δ	- Control deflection angle
$\lambda_{1,2}$	- Damping exponent; real part of $m_{1,2}$
ξ	- Complex total angle of attack
τ	- Defined by Equation 103
ψ_o	- Angle of oscillatory plane in the $\bar{\alpha} - \bar{\beta}$ plane
ψ	- Angle of the K arm in complex plane with respect to $\bar{\alpha}$ axis
$\omega_{1,2}$	- Nutation and precession frequencies; imaginary parts of $m_{1,2}$
Ω	- Total angular velocity

A DETAILED DEVELOPMENT OF THE TRICYCLIC THEORY

Introduction

The Tricyclic Theory is a solution to the aeroballistic equations of motion which makes use of complex variables. It is the <u>only</u> theory that describes the free-flight motion of a rolling vehicle in a relatively complete manner. It has the unique ability to predict the motion of a vehicle quantitatively as planar, elliptical, epicyclical or tricyclical, depending on the physical and aerodynamic characteristics of the vehicle. Consequently, it is important that flight dynamicists be able to apply the theory in predicting and analyzing the motion of free flight vehicles. It is equally important that flight dynamicists realize the restrictions inherent in the theory, most of which stem from the fact that the theory is based on a solution to a linear differential equation, which inherently has the assumptions of constant coefficients and small angles. However, properly applied, the theory is a very useful tool in analyzing flight dynamics problems.

The first step in deriving the Tricyclic Theory is to derive the aeroballistic equations of motion.

Aeroballistic Equations of Motion

The Tricyclic Theory is based on the aeroballistic axis system and the resulting equations of motion. Since there may be some confusion involved in the differences between some of the various axis systems (i.e., body fixed, aeroballistic and precessing aeroballistic) the aeroballistic set of moment equations is derived and discussed in detail.

The equations of motion are based on Newton's statement that the time rate of change of linear momentum must equal the sum of applied forces

$$\sum_{i=1}^{\infty} \vec{f} = \sum_{i=1}^{\infty} \frac{d}{dt} (m_i \vec{v}_i) \ , \tag{1}$$

where m is the elemental mass and $\vec{f}$ is the elemental force. The moment can be obtained by simply multiplying by the distance $\vec{r}$ to the elemental mass and summing elemental moments

$$\vec{M} = \sum \vec{r} \times \vec{f} = \sum \frac{d}{dt} (m\vec{r} \times \vec{v}) \ , \tag{2}$$

but the vector velocity $\vec{v}$ of the elementary particle m is also the angular velocity times $\vec{r}$. Consequently

$$\vec{v} = \vec{\omega} \times \vec{r} \ . \tag{3}$$

Substituting

$$\vec{M} = \sum \frac{d}{dt}\left[m\vec{r} \times (\vec{\omega} \times \vec{r})\right] \ , \tag{4}$$

which from vector analysis can be written

$$\vec{M} = \sum \frac{d}{dt} m\left[(\vec{r} \cdot \vec{r})\vec{\omega} - \vec{r}(\vec{r} \cdot \vec{\omega})\right] \tag{5}$$

$$\vec{M} = \frac{d}{dt}\left\{\left(\sum mr^2\right)\vec{\omega} - \sum m\vec{r}(\vec{r} \cdot \vec{\omega})\right\} \ . \tag{6}$$

At this point it is tempting to take a giant step forward by simply noting that $\sum mr^2$ is the moment of inertia and that $\sum m\vec{r}(\vec{r} \cdot \vec{\omega})$ is equivalent to the product of inertia times the angular velocity. However, the derivation will be done in detail. Similar developments are found in References 4, 5, 6 and many others. To accomplish this we will resort to the Cartesian coordinate system shown in Figure 1. Since $\vec{r}$ is a vector it can be written as

$$\vec{r} = x\vec{i} + y\vec{j} + z\vec{k} \tag{7}$$

and

$$r^2 = x^2 + y^2 + z^2 \ , \tag{8}$$

where $\vec{i}$, $\vec{j}$, and $\vec{k}$ are unit vectors and the angular velocity vector $\vec{\omega}$, which is not necessarily coincident with $\vec{r}$, is

$$\vec{\omega} = \omega_x\vec{i} + \omega_y\vec{j} + \omega_z\vec{k} \tag{9}$$

If we substitute (7), (8) and (9) into (6) we have

$$\vec{M} = \frac{d}{dt}\left\{\sum m(x^2 + y^2 + z^2)(\omega_x\vec{i} + \omega_y\vec{j} + \omega_z\vec{k}) - \sum m(x\vec{i} + y\vec{j} + z\vec{k})(x\omega_x + y\omega_y + z\omega_z)\right\} \tag{10}$$

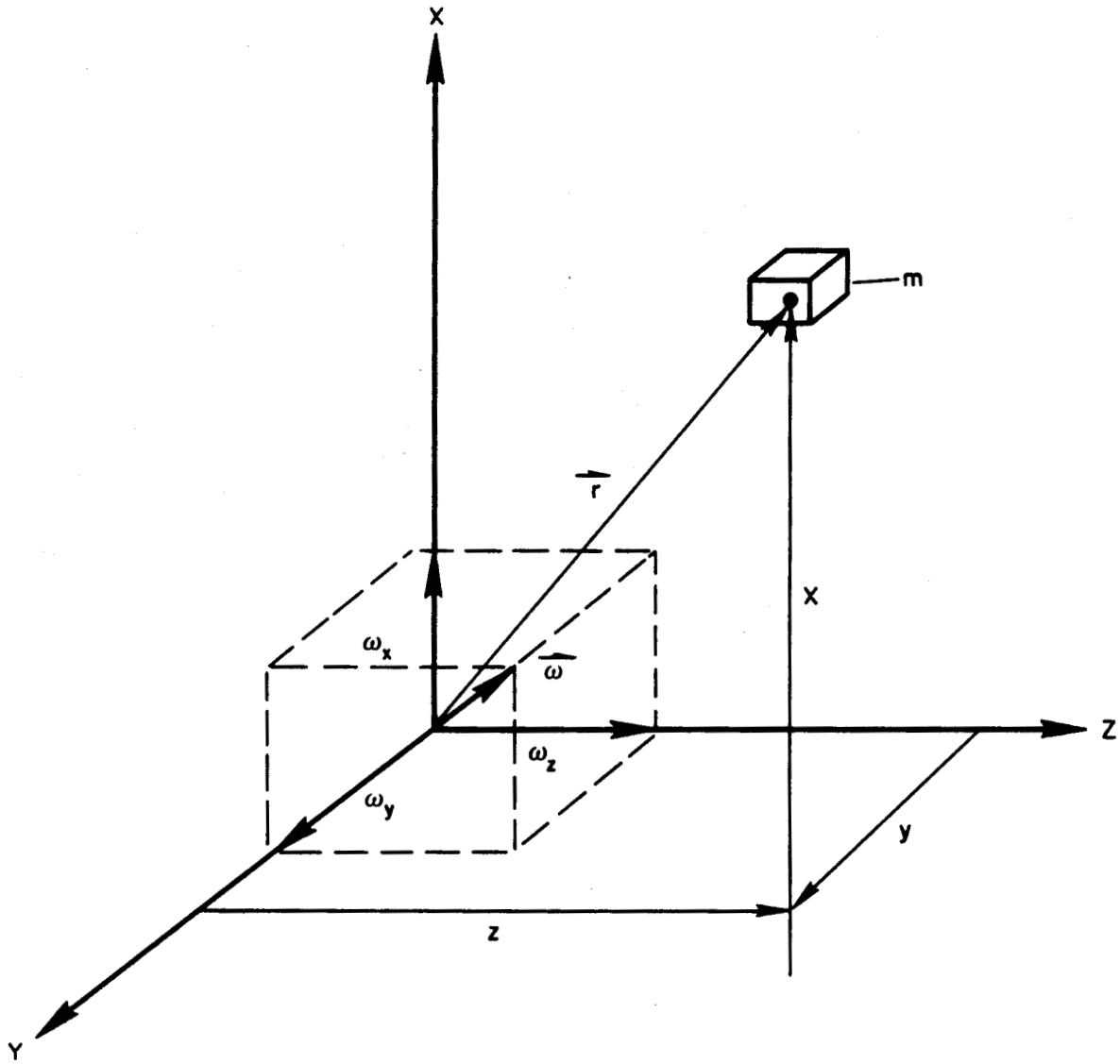

Figure 1. Inertial Axis System

and

$$\vec{M} = \frac{d}{dt}\left\{\sum m\left[\omega_x(x^2 + y^2 + z^2) - (\omega_x x^2 + \omega_y xy + \omega_z xz)\right]\vec{i}\right.$$

$$+\sum m\left[\omega_y(x^2 + y^2 + z^2) - (\omega_x xy + \omega_y y^2 + \omega_z yz)\right]\vec{j} \tag{11}$$

$$\left.+\sum m\left[\omega_z(x^2 + y^2 + z^2) - (\omega_x xz + \omega_y yz + \omega_z z^2\right]\vec{k}\right\} .$$

The scalar moments about the three inertial axes X, Y, and Z, which are fixed in space are obtained by taking the $\vec{i}$, $\vec{j}$, $\vec{k}$ components, which are

$$M_x = \frac{d}{dt}\left[\sum m\left[\omega_x(y^2 + z^2) - \omega_y xy - \omega_z xz\right]\right] \tag{12}$$

$$M_y = \frac{d}{dt}\left[\sum m\left[\omega_y(x^2 + z^2) - \omega_x xy - \omega_z yz\right]\right] \tag{13}$$

$$M_z = \frac{d}{dt}\left[\sum m\left[\omega_z(x^2 + y^2) - \omega_x xz - \omega_y yz\right]\right] . \tag{14}$$

Now it can be seen that the terms involving $\sum m(y^2 + z^2)$, $\sum m(x^2 + z^2)$, $\sum m(x^2 + y^2)$ are moments of inertia I about the X, the Y, and the Z axis respectively and that the remaining terms involve product of inertia. For instance $\sum mxy$ is the product of inertia about the Z axis and is denoted as I_{xy}. Therefore

$$M_x = \frac{d}{dt}(I_{xx}\omega_x - I_{xy}\omega_y - I_{xz}\omega_z) \tag{15}$$

$$M_y = \frac{d}{dt}(I_{yy}\omega_y - I_{xy}\omega_x - I_{yz}\omega_z) \tag{16}$$

$$M_z = \frac{d}{dt}(I_{zz}\omega_z - I_{xz}\omega_x - I_{yz}\omega_y) . \tag{17}$$

This set of equations, which are the moments about the X, Y, and Z axes when they are <u>fixed</u> in space, are often written as simply

$$\vec{M} = \frac{d}{dt}(I\vec{\omega}), \tag{18}$$

where I includes all the moments of inertia and products of inertia and $\vec{\omega}$ includes all the angular velocities of the body (ω_x, ω_y, ω_z). Also $I\vec{\omega}$ is the angular momentum $\vec{H}$; consequently

$$\frac{d\vec{H}}{dt} = \vec{M} = \frac{d}{dt}(I\vec{\omega}) \ , \tag{19}$$

where

$$\vec{H} = I\vec{\omega} \ . \tag{20}$$

Equation 19 is important since it says that the applied moments are equal to the time rate of change of moment of momentum, which is the angular momentum. Unfortunately, Equation 19 refers to an axis system fixed in space where an axis system free to move in a specified manner with respect to an axis system fixed in space is needed to describe the motion of a body. This extension was done by Euler. Referring to Figure 2 we have a moving axis system x, y, z referred to an inertially fixed axis system X Y Z, and $\vec{H}$ and $\vec{\omega}$ denote the total moment of momentum vector and $\vec{\omega}$ the total angular velocity vector of the body. Therefore

$$\vec{\omega} = \omega_x\vec{i} + \omega_y\vec{j} + \omega_z\vec{k} \tag{21}$$

$$\vec{H} = H_x\vec{i} + H_y\vec{j} + H_z\vec{k} \ , \tag{22}$$

where $\vec{i}\ \vec{j}\ \vec{k}$ are unit vectors, which are regarded as position vectors indicating the position of the xyz axes. Then from Equation 19 the moment for the moving axis system

$$\vec{M} = \frac{d\vec{H}}{dt} = \vec{i}\frac{dH_x}{dt} + \vec{j}\frac{dH_y}{dt} + \vec{k}\frac{dH_z}{dt} + H_x\frac{d\vec{i}}{dt} + H_y\frac{d\vec{j}}{dt} + H_z\frac{d\vec{k}}{dt} \ , \tag{23}$$

since $\vec{i}$, $\vec{j}$ and $\vec{k}$ change in the moving axis system. From vector analysis

$$\frac{d\vec{i}}{dt} = \vec{\omega} \times \vec{i} = \begin{vmatrix} \vec{i} & \vec{j} & \vec{k} \\ \omega_x & \omega_y & \omega_z \\ 1 & 0 & 0 \end{vmatrix} = \omega_z\vec{j} - \omega_y\vec{k} \tag{24}$$

$$\frac{d\vec{j}}{dt} = \vec{\omega} \times \vec{j} = \begin{vmatrix} \vec{i} & \vec{j} & \vec{k} \\ \omega_x & \omega_y & \omega_z \\ 0 & 1 & 0 \end{vmatrix} = -\omega_z\vec{i} + \omega_x\vec{k} \tag{25}$$

$$\frac{d\vec{k}}{dt} = \vec{\omega} \times \vec{k} = \begin{vmatrix} \vec{i} & \vec{j} & \vec{k} \\ \omega_x & \omega_y & \omega_z \\ 0 & 0 & 1 \end{vmatrix} = \omega_y\vec{i} - \omega_x\vec{j} \ . \tag{26}$$

Substituting these derivatives in Equation 23 yields

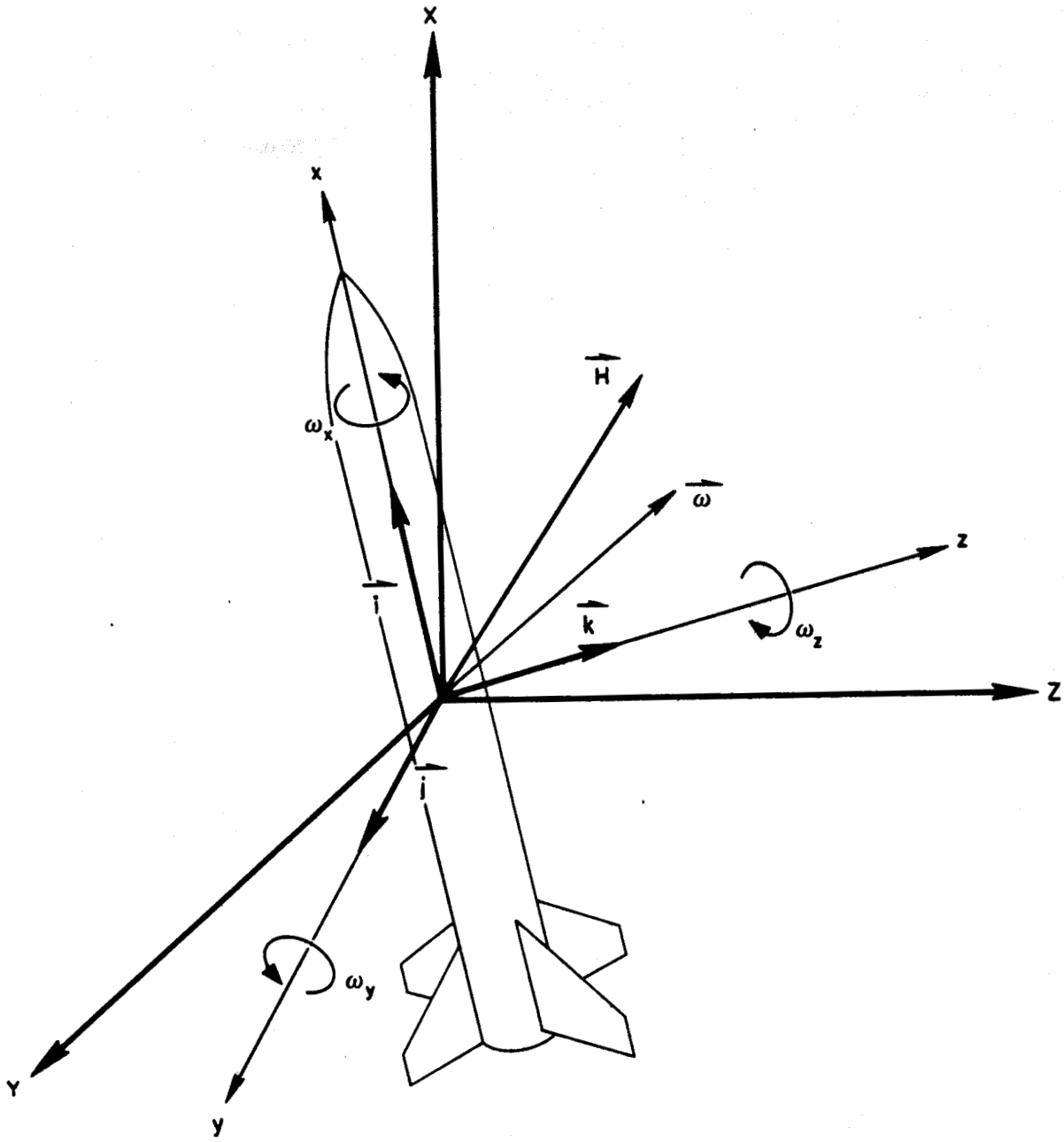

Figure 2. Axis System

$$\frac{d\vec{H}}{dt} = \left(\frac{dH_x}{dt} - H_y\omega_z + H_z\omega_y\right)\vec{i}$$

$$+\left(\frac{dH_y}{dt} + H_x\omega_z - H_z\omega_x\right)\vec{j} \tag{27}$$

$$+\left(\frac{dH_z}{dt} - H_x\omega_y + H_y\omega_x\right)\vec{k} \quad .$$

Since

$$\frac{d\vec{H}}{dt} = \vec{M} = M_x\vec{i} + M_y\vec{j} + M_z\vec{k} \tag{28}$$

the moments about the x, y and z axes are

$$M_x = \frac{dH_x}{dt} + H_z\omega_y - H_y\omega_z \tag{29}$$

$$M_y = \frac{dH_y}{dt} + H_x\omega_z - H_z\omega_x \tag{30}$$

$$M_z = \frac{dH_z}{dt} + H_y\omega_x - H_x\omega_y \quad , \tag{31}$$

where H_x, H_y, and H_z are obtained from (15), (16), and (17)

$$H_x = I_{xx}\omega_x - I_{xy}\omega_y - I_{xz}\omega_z \tag{32}$$

$$H_y = I_{yy}\omega_y - I_{xy}\omega_x - I_{yz}\omega_z \tag{33}$$

$$H_z = I_{zz}\omega_z - I_{xz}\omega_x - I_{yz}\omega_y \quad . \tag{34}$$

Equations 29 through 34 are the complete equations for a body in a moving axis system. However, they are in an inconvenient form which is difficult to use. A better form can be obtained by noting from (23), (24), (25) and (26) that the total moment vector can be expressed as

$$\vec{M} = \frac{d\vec{H}}{dt} + \vec{\Omega} \times \vec{H} \ , \tag{35}$$

where $\vec{\Omega}$ is the total angular velocity of the moving axes x, y, z. And recalling (19) and (20),

$$\vec{M} = \frac{d}{dt}(I\vec{\omega}) + \vec{\Omega} \times I\vec{\omega} \ . \tag{36}$$

Completing the differentiation

$$\vec{M} = I\dot{\vec{\omega}} + \dot{I}\vec{\omega} + \vec{\Omega} \times I\vec{\omega} \ , \tag{37}$$

which is the complete general equation. Expressed in matrix form this equation becomes

$$\begin{vmatrix} M_x \\ M_y \\ M_z \end{vmatrix} = \begin{vmatrix} I_{xx} & -I_{xy} & -I_{xz} \\ -I_{yx} & I_{yy} & -I_{yz} \\ -I_{zx} & -I_{zy} & I_{zz} \end{vmatrix} \begin{vmatrix} \dot{\omega}_x \\ \dot{\omega}_y \\ \dot{\omega}_z \end{vmatrix} + \begin{vmatrix} \dot{I}_{xx} & -\dot{I}_{xy} & -\dot{I}_{xz} \\ -\dot{I}_{yx} & \dot{I}_{yy} & -\dot{I}_{yz} \\ -\dot{I}_{yx} & -\dot{I}_{zy} & \dot{I}_{zz} \end{vmatrix} \begin{vmatrix} \omega_x \\ \omega_y \\ \omega_z \end{vmatrix} \tag{38}$$

$$+ \begin{vmatrix} \Omega_x \\ \Omega_y \\ \Omega_z \end{vmatrix}^* \times \begin{vmatrix} I_{xx} & -I_{xy} & -I_{xz} \\ -I_{yx} & I_{yy} & -I_{yz} \\ -I_{zx} & -I_{zy} & I_{zz} \end{vmatrix} \begin{vmatrix} \omega_x \\ \omega_y \\ \omega_z \end{vmatrix} \ .$$

Now the symbols are replaced with symbols normally used in aerodynamics

$$\begin{vmatrix} L \\ M \\ N \end{vmatrix} = \begin{vmatrix} I_{xx} & -I_{xy} & -I_{xz} \\ -I_{yx} & I_{yy} & -I_{yz} \\ -I_{zx} & -I_{zy} & I_{zz} \end{vmatrix} \begin{vmatrix} \dot{p} \\ \dot{q} \\ \dot{r} \end{vmatrix} + \begin{vmatrix} \dot{I}_{xx} & -\dot{I}_{xy} & -\dot{I}_{xz} \\ -\dot{I}_{yx} & \dot{I}_{yy} & -\dot{I}_{yz} \\ -\dot{I}_{zx} & -\dot{I}_{zy} & \dot{I}_{zz} \end{vmatrix} \begin{vmatrix} p \\ q \\ r \end{vmatrix} \tag{39}$$

$$+ \begin{vmatrix} p \\ q \\ r \end{vmatrix}^* \times \begin{vmatrix} I_{xx} & -I_{xy} & -I_{xz} \\ -I_{yx} & I_{yy} & -I_{yz} \\ -I_{zx} & -I_{zy} & I_{zz} \end{vmatrix} \begin{vmatrix} p \\ q \\ r \end{vmatrix} \ ,$$

where L, M, and N are roll, pitch, and yaw moments, and p, q, and r are roll, pitch, and yaw angular velocities (see Figure 3).

Equation 39 is the complete set of moment equations for three degrees of angular freedom (ψ, θ, and ϕ) in matrix form; when the matrix algebra is completed, this equation can provide the three moment equations for a body fixed axis system. Equation 39 can be used to derive the moment equations for any type of axis system depending on the angular rates substituted for p, q, and r in the matrix marked with an asterisk since this matrix controls the rate at which the axis system moves. For the aeroballistic system, p is made zero in this matrix since it is a non-rolling axis system. Furthermore, the tricyclic theory assumes that products of inertia and rates of change of inertia are zero. This results in the following version of (39)

$$\begin{vmatrix} L \\ M \\ N \end{vmatrix} = \begin{vmatrix} I_{xx} & 0 & 0 \\ 0 & I_{yy} & 0 \\ 0 & 0 & I_{zz} \end{vmatrix} \begin{vmatrix} \dot{p} \\ \dot{q} \\ \dot{r} \end{vmatrix} + \begin{vmatrix} 0 \\ q \\ r \end{vmatrix} \times \begin{vmatrix} I_{xx} & 0 & 0 \\ 0 & I_{yy} & 0 \\ 0 & 0 & I_{zz} \end{vmatrix} \begin{vmatrix} p \\ q \\ r \end{vmatrix} , \tag{40}$$

which is manipulated in this manner:

$$\begin{vmatrix} L \\ M \\ N \end{vmatrix} = \begin{vmatrix} I_{xx}\dot{p} & 0 & 0 \\ 0 & I_{yy}\dot{q} & 0 \\ 0 & 0 & I_{zz}\dot{r} \end{vmatrix} + \begin{vmatrix} 0 \\ q \\ r \end{vmatrix} \times \begin{vmatrix} I_{xx}p & 0 & 0 \\ 0 & I_{yy}q & 0 \\ 0 & 0 & I_{zz}r \end{vmatrix} \tag{41}$$

$$\begin{vmatrix} L \\ M \\ N \end{vmatrix} = \begin{vmatrix} I_{xx}\dot{p} \\ I_{yy}\dot{q} \\ I_{zz}\dot{r} \end{vmatrix} + \begin{vmatrix} i & j & k \\ 0 & q & r \\ I_{xx}p & I_{yy}q & I_{zz}r \end{vmatrix}$$

$$\begin{aligned} L &= I_{xx}\dot{p} + qrI_{zz} - qrI_{yy} \\ M &= I_{yy}\dot{q} + rpI_{xx} \\ N &= I_{zz}\dot{r} - qpI_{xx} \quad , \end{aligned} \tag{42}$$

and substituting by virtue of symmetry

$$I = I_{yy} = I_{zz}$$

$$I_{xx} = I_x \ .$$

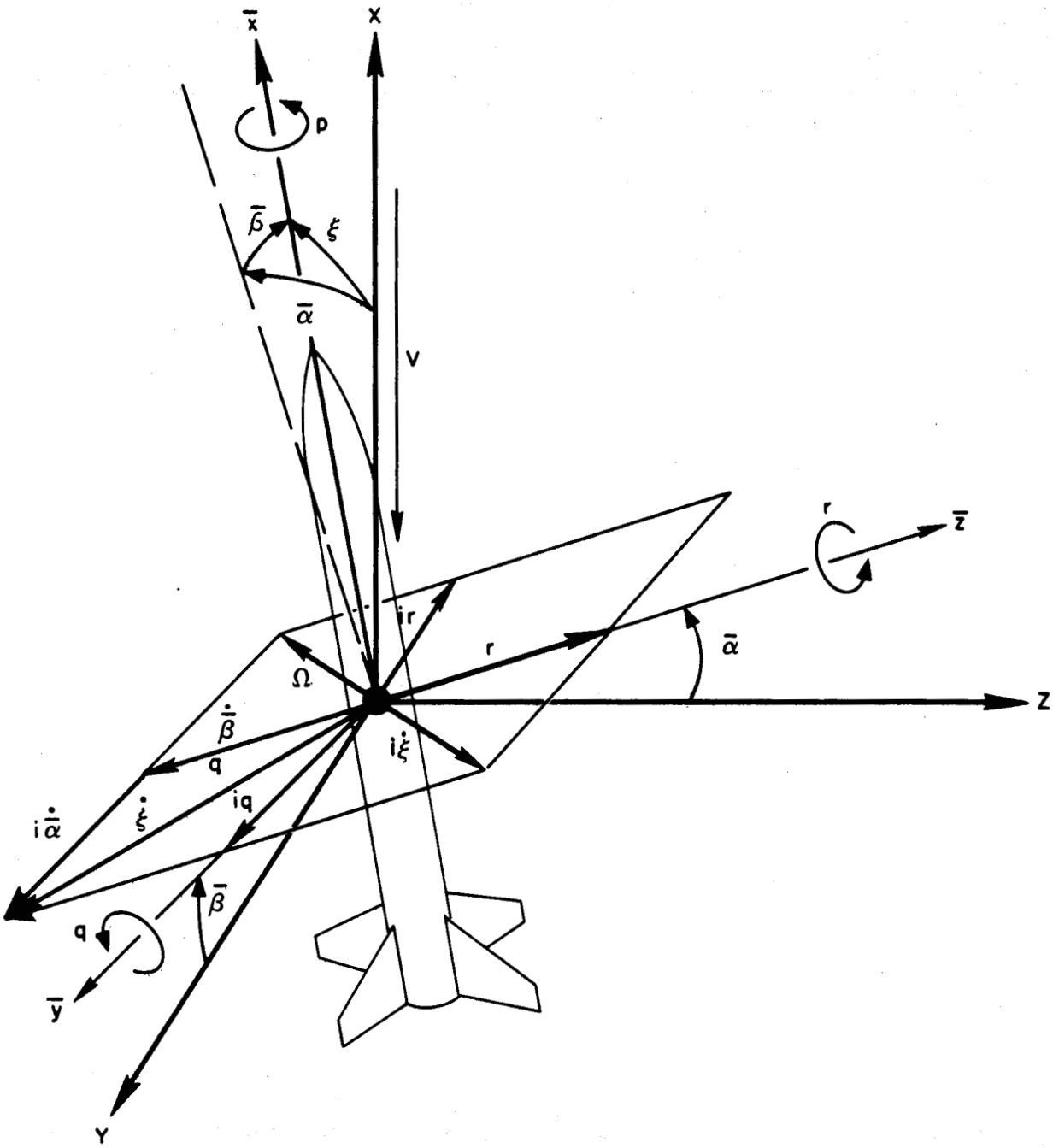

Figure 3. Aeroballistic System

The equations for the sum of inertial moments about the x, y, and z axes result:

$$L = I_x \dot{p} \tag{43}$$

$$M = I\dot{q} + rpI_x \tag{44}$$

$$N = I\dot{r} - qpI_x \ , \tag{45}$$

which are the aeroballistic equations. It should be emphasized that, while the body is rolling at the rate of p, the axis system is not rolling.

Tricyclic Solution to Aeroballistic Equations

To obtain an analytic solution to the three aeroballistic equations it is necessary to decouple the roll equation from the pitch and yaw equations, which is done by assuming the roll rate p to be constant. The effects of this assumption, as well as others made during the course of this theoretical development, on the accuracy of application of the theory is discussed in the section entitled Application. This assumption then leaves Equation 44 and 45 to be solved. The first step is to define the applied aerodynamic moments M and N and equate them to the inertial moments on the right side of the equations. Since this problem is complicated enough in its simplest form we will consider only those moments due to q, r, $\dot{\alpha}$, $\dot{\beta}$, α, and β, plus Magnus moment resulting from combined roll rate and angle of attack (which is only one of the several complex moments that can be considered).

$$M_{p\beta} = C_{mp\beta} q' \frac{Sd^2}{2V} \tag{46}$$

$$N_{p\alpha} = C_{np\alpha} q' \frac{Sd^2}{2V} \tag{47}$$

Magnus moments

$$M_{\alpha} = C_{m\alpha} q' Sd \tag{48}$$

$$N_{\beta} = C_{n\beta} q' Sd \tag{49}$$

Static stability moments

$$M_q = \frac{C_{mq} q' Sd^2}{2V} \tag{50}$$

$$N_r = \frac{C_{nr} q' Sd^2}{2V} \tag{51}$$

Damping moments

$$M_{\dot{\alpha}} = \frac{C_{m\dot{\alpha}} q' S d^2}{2V} \tag{52}$$

Aerodynamic lag moments

$$N_{\dot{\beta}} = \frac{C_{n\dot{\beta}} q' S d^2}{2V} \quad . \tag{53}$$

In addition to these moments, which are normally associated with a symmetrical vehicle, a moment due to control deflection or an aerodynamic asymmetry must be added. Since a moment associated with an aerodynamic asymmetry is fixed in the rolling body axis, we must break it up into components around the $\bar{y}$ and $\bar{z}$ aeroballistic axes. This can be accomplished by realizing that the roll orientation of the body is simply a function of pt since p is treated as a constant. Consequently, we can represent the two components of the moments due to asymmetries (or control deflection) as

$$M_\delta \ \delta \cos pt \quad \text{and} \quad M_\delta \ \delta \sin pt \ .$$

When all of these applied moments are substituted in Equations 44 and 45, the complete pair of equations to be solved is

$$I\dot{q} + rpI_x - M_\alpha \bar{\alpha} - M_q q - M_{\dot{\alpha}} \dot{\bar{\alpha}} - M_\delta \ \delta \cos pt - M_{p\beta} p\bar{\beta} = 0 \tag{54}$$

$$I\dot{r} - qpI_x - N_\beta \bar{\beta} - N_r r - N_{\dot{\beta}} \dot{\bar{\beta}} - M_\delta \ \delta \sin pt - N_{p\alpha} p\bar{\alpha} = 0 \ , \tag{55}$$

where Equation 54 is the sum of the moments about the $\bar{y}$ axis and Equation 55 is the sum of the moments about the $\bar{z}$ axis. The aeroballistic axis system is shown in Figure 3, where the various angles and their time derivatives are pictorially demonstrated. Equations 54 and 55 are scalar equations, and the quantities in Figure 3 are scalars (although complex) even though their direction is demonstrated by arrows. The complex angle of attack ξ is defined as a complex quantity composed of the two angles $\bar{\alpha}$ and $\bar{\beta}$

$$\xi = i\bar{\alpha} + \bar{\beta} \ , \tag{56}$$

where ξ is identical to $\vec{\alpha}$ used in Nicolaides' original treatment. The symbol is changed in an effort to avoid confusion. The i simply denotes that $\bar{\alpha}$ is perpendicular to $\bar{\beta}$. It should be noted that $\bar{\alpha}$ and $\bar{\beta}$ are positive when measured from the body $\bar{x}$ axis to the flight path, which is opposite in sense to the usual aeroballistic angle of attack $\tilde{\alpha}$ and $\tilde{\beta}$ used later in the report and obtained from a 6 DOF calculation (see Figure 8). Notice that the position of the body $\bar{x}$ axis is defined by

the two angles $\bar{\alpha}$ and $\bar{\beta}$ and that angular rates of the $\bar{y}$ and $\bar{z}$ axes is defined by q and r. The axis system does not rotate about the $\bar{x}$ axis, but the body does roll about the $\bar{x}$ axis with the constant rate p. The angular rate q is represented by an arrow perpendicular to the $\bar{\alpha}$ plane, and r is represented by an arrow perpendicular to $\bar{\beta}$. From Figure 3 it is possible to see that

$$q = \dot{\bar{\alpha}}, \quad \dot{q} = \ddot{\bar{\alpha}}$$

$$r = -\dot{\bar{\beta}}, \; \dot{r} = -\ddot{\bar{\beta}} \; . \tag{57}$$

All of the angular velocities in the figure are vectors in the sense that they can be represented by arrows with a direction perpendicular to the plane of the angle. It should also be noted that Ω($\vec{q}$ in Nicolaides' terminology) can be expressed in complex fashion as

$$\Omega = q + ir \; . \tag{58}$$

It is now becoming clear that the complex plane has been chosen perpendicular to the $\bar{x}$ axis and in fact is coincident with $\bar{\alpha}$, $\bar{\beta}$, ξ, $\dot{\bar{\alpha}}$, $\dot{\bar{\beta}}$, $\dot{\xi}$, q, r, Ω, and the $\bar{y}$ and $\bar{z}$ axes. This is a tremendous advantage in reducing the equations to a solvable form. A vertical view of this complex plane is shown in Figure 4. Now we can easily see the rest of the relations:

$$\Omega = -i\dot{\xi} \tag{59}$$

$$\xi = i\bar{\alpha} + \bar{\beta} \tag{60}$$

$$\dot{\xi} = i\dot{\bar{\alpha}} + \dot{\bar{\beta}} \tag{61}$$

$$\Omega = -\, i\,(i\dot{\bar{\alpha}} + \dot{\bar{\beta}}) = \dot{\bar{\alpha}} - i\dot{\bar{\beta}} = -\, i\dot{\xi} \; . \tag{62}$$

With these relations we are ready to manipulate Equations 54 and 55 so that they can be solved simultaneously. By multiplying one of the moment equations by i the problem is shifted into the complex plane. Then the two equations are added to get the total moment equation in the complex plane which can be solved in terms of a single complex angle ξ. Multiplying (55) by i

$$I\dot{q} + rpI_x - M_\alpha \bar{\alpha} - M_q q - M_{\dot{\alpha}} \dot{\bar{\alpha}} - M_\delta \delta \cos pt - M_{p\beta} p\bar{\beta} = 0 \tag{63}$$

$$iI\dot{r} - iqpI_x - iN_\beta \bar{\beta} - iN_r r - iN_{\dot{\beta}} \dot{\bar{\beta}} - iM_\delta \delta \sin pt - iN_{p\alpha} p\bar{\alpha} = 0 \; , \tag{64}$$

and adding the two equations and collecting terms yields

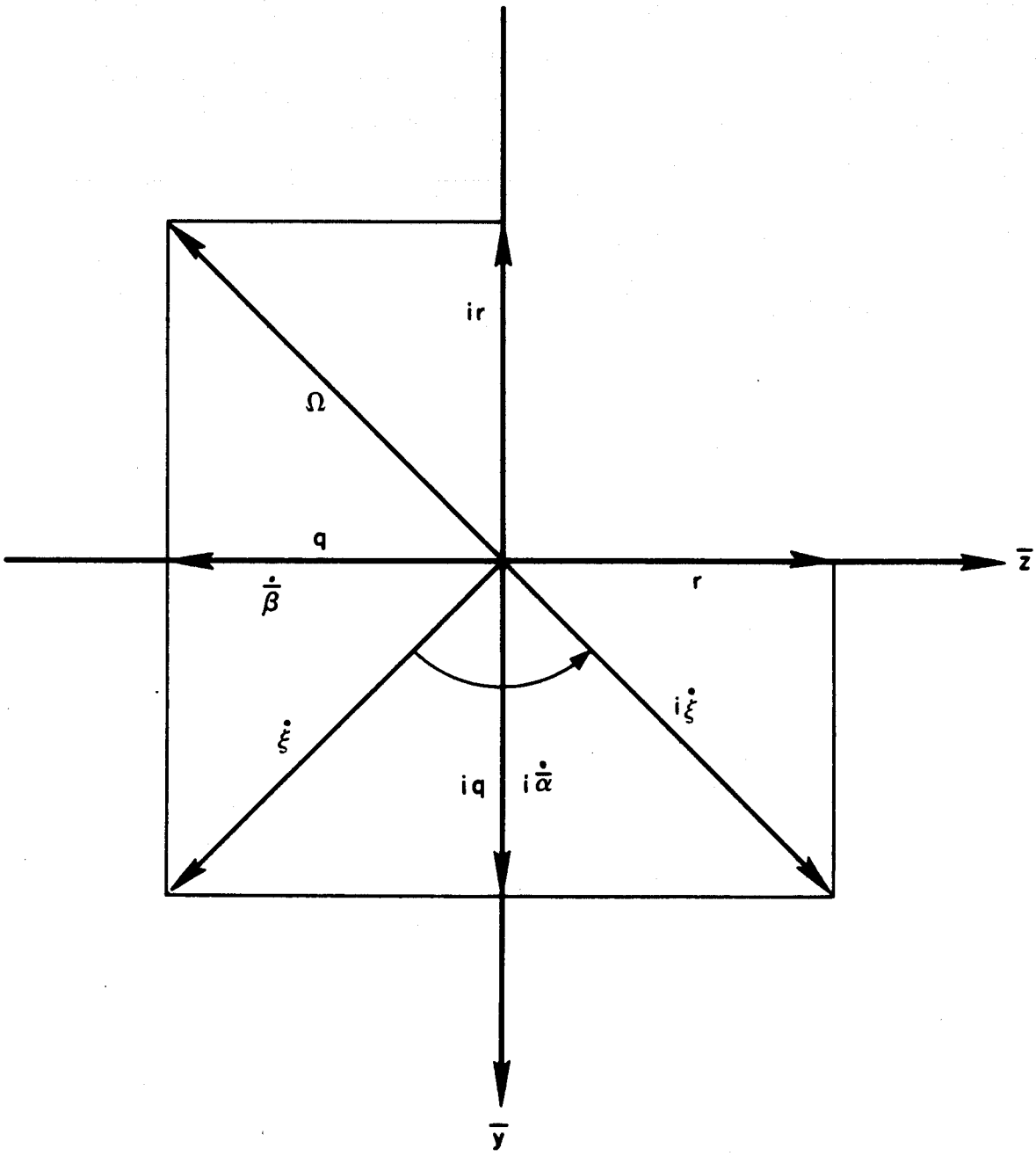

Figure 4. Complex Plane

$$I(\dot{q} + i\dot{r}) - I_x p(iq - r) - M_\alpha \bar{\alpha} - iN_\beta \bar{\beta} - M_q q - iN_r r$$

$$- M_{\dot{\alpha}} \dot{\bar{\alpha}} - iN_{\dot{\beta}} \dot{\bar{\beta}} - M_\delta \delta (\cos pt + i \sin pt) - M_{p\beta} p\bar{\beta} - iN_{p\alpha} p\bar{\alpha} = 0 \quad . \tag{65}$$

Now if the vehicle is rotationally symmetrical, the static and dynamic stability derivatives about the $\bar{y}$ axis are equal to the stability derivatives about the $\bar{z}$ axis. Consequently

$$M_\alpha = -N_\beta, \; M_q = N_r, \; M_{\dot{\alpha}} = -N_{\dot{\beta}}, \; M_{p\beta} = N_{p\alpha} \quad . \tag{66}$$

Using the normal symbols for moments about the $\bar{y}$ axis (i.e., M_α, M_q, $M_{\dot{\alpha}}$), Equation 65 becomes

$$I(\dot{q} + i\dot{r}) - I_x p(iq - r) - M_\alpha(\alpha - i\beta) - M_q(q + ir)$$

$$- M_{\dot{\alpha}}(\dot{\bar{\alpha}} - i\dot{\bar{\beta}}) - M_\delta \delta (\cos pt + i \sin pt) - M_{p\beta} p(i\bar{\alpha} + \bar{\beta}) = 0 \quad . \tag{67}$$

Since the equation must be in terms of ξ, the total angle of attack, Equations 56 through 62 can be used to substitute for $\bar{\alpha}$, $\bar{\beta}$, $\dot{\bar{\alpha}}$, $\dot{\bar{\beta}}$, q, r, $\dot{q}$, and $\dot{r}$ in Equation 67 as follows:

$$\dot{q} + i\dot{r} = \dot{\Omega} = \frac{d}{dt}(- i\dot{\xi}) = -i\ddot{\xi} \qquad [\text{from (58) and (59)}]$$

$$iq - r = i\dot{\bar{\alpha}} + \dot{\bar{\beta}} = \dot{\xi} \qquad [\text{from (57) and (61)}]$$

$$\bar{\alpha} - i\bar{\beta} = \frac{i^2}{i^2}(\bar{\alpha} - i\bar{\beta}) = \frac{i}{i^2}(i\bar{\alpha} - i^2\bar{\beta}) = -i(i\bar{\alpha} + \bar{\beta}) = -i\xi \qquad [\text{from (60)}]$$

$$q + ir = \Omega = -i\dot{\xi} \qquad [\text{from (59) and (59)}]$$

$$\dot{\bar{\alpha}} - i\dot{\bar{\beta}} = -i\dot{\xi} \qquad [\text{from (62)}] \quad .$$

Equation 67 becomes

$$I(- i\ddot{\xi}) - I_x p(\dot{\xi}) - M_\alpha(- i\xi) - M_q(- i\xi) - M_{\dot{\alpha}}(- i\dot{\xi}) - M_\delta \delta(\cos pt + i \sin pt) - M_{p\beta} p\xi = 0 \quad . \tag{69}$$

Multiplying by $\frac{i}{I}$

$$\ddot{\xi} - ip\frac{I_x}{I}\dot{\xi} - \frac{M_\alpha}{I}\xi - \frac{M_q}{I}\dot{\xi} - \frac{M_{\dot{\alpha}}}{I}\dot{\xi} - \frac{iM_\delta}{I}\delta(i \sin pt + \cos pt) - ip\frac{M_{p\beta}}{I}\xi = 0 \quad . \tag{70}$$

Collecting terms

$$\ddot{\xi} + \left(-ip\frac{I_x}{I} - \frac{M_q + M_{\dot{\alpha}}}{I}\right)\dot{\xi} + \left(-ip\frac{M_{p\beta}}{I} - \frac{M_\alpha}{I}\right)\xi$$

$$- \frac{M_\delta}{I}\,\delta\,(-\sin pt + i\cos pt) = 0 \quad . \tag{71}$$

Now

$$-\sin pt + i\cos pt = -\left[-i\left(\frac{e^{ipt} - e^{-ipt}}{2}\right)\right] + i\left(\frac{e^{ipt} + e^{-ipt}}{2}\right)$$

$$= \frac{ie^{ipt} - ie^{-ipt} + ie^{ipt} + ie^{-ipt}}{2} = ie^{ipt} \quad .$$

Consequently Equation 71 becomes

$$\ddot{\xi} + \left(-ip\frac{I_x}{I} - \frac{M_q + M_{\dot{\alpha}}}{I}\right)\dot{\xi} + \left(-ip\frac{M_{p\beta}}{I} - \frac{M_\alpha}{I}\right)\xi = \frac{iM_\delta}{I}\,\delta\,e^{ipt} \quad . \tag{72}$$

We can replace the coefficients with

N_1, N_2 and N_3, which are <u>constants</u>:

$$N_1 = \left(-ip\frac{I_x}{I} - \frac{M_q + M_{\dot{\alpha}}}{I}\right) \tag{73}$$

$$N_2 = \left(-ip\frac{M_{p\beta}}{I} - \frac{M_\alpha}{I}\right) \tag{74}$$

$$N_3 = i\left(\frac{M_\delta}{I}\,\delta\right) \quad . \tag{75}$$

This yields

$$\ddot{\xi} + N_1\dot{\xi} + N_2\xi = N_3\,e^{ipt} \,, \tag{76}$$

which is a linear, second order differential equation with constant coefficients which can be solved. The homogenous part of the equation is

$$\ddot{\xi} + N_1\dot{\xi} + N_2\xi = 0 \,. \tag{77}$$

The auxiliary equation of (77) is

$$m^2 + N_1 m + N_2 = 0 \ .$$

The two roots of the equation are obtained from the following algebraic manipulation:

$$m^2 + N_1 m = -N_2$$

$$m^2 + N_1 m + \left(\frac{N_1}{2}\right)^2 = \left(\frac{N_1}{2}\right)^2 - N_2$$

$$\left(m + \frac{N_1}{2}\right)^2 = \left(\frac{N_1}{2}\right)^2 - N_2$$

$$m + \frac{N_1}{2} = \pm\sqrt{\left(\frac{N_1}{2}\right)^2 - N_2}$$

$$m = -\frac{N_1}{2} \pm\sqrt{\left(\frac{N_1}{2}\right)^2 - N_2} \ ,$$

but since m is actually two separate quantities, m is replaced by $m_{1,2}$:

$$m_{1,2} = -\frac{N_1}{2} \pm\sqrt{\left(\frac{N_1}{2}\right)^2 - N_2} \ , \tag{78}$$

where m_1 involves the positive radical, m_2 involves the negative radical, and they are both complex values. The symbol m is identical to Φ in Nicolaides' notation. It was changed to avoid confusion with the symbol for roll angle. The general solution to the homogeneous part of the equation is known to be

$$\xi_H = K_1 e^{m_1 t} + K_2 e^{m_2 t} \ . \tag{79}$$

To complete the solution the particular integral is evaluated:

$$\xi_p = e^{m_2 t} \int \left[e^{(m_1 - m_2)t} \int e^{-m_1 t} N_3 e^{ipt} dt \right] dt \ . \tag{80}$$

Integrating

$$\xi_p = e^{m_2 t} \int \left[e^{(m_1 - m_2)t} \left(\frac{N_3}{-m_1 + ip} \right) e^{(-m_1 + ip)t} \right] dt$$

$$\xi_p = \frac{N_3 e^{m_2 t}}{(-m_1 + ip)} \int e^{(-m_2 + ip)t} dt$$

$$\xi_p = \frac{N_3 e^{m_2 t}}{(-m_1 + ip)} \left[\frac{e^{(-m_2 + ip)t}}{-m_2 + ip} \right]$$

$$\xi_p = \frac{N_3 e^{ipt}}{(ip - m_1)(ip - m_2)} \tag{81}$$

$$\xi_p = K_3 e^{ipt} \quad , \tag{82}$$

where

$$K_3 = \frac{N_3}{(ip - m_1)(ip - m_2)} \tag{83}$$

The complete solution is simply the sum of (79) and (82), which is

$$\xi = K_1 e^{m_1 t} + K_2 e^{m_2 t} + K_3 e^{ipt} \quad , \tag{84}$$

where K_1 and K_2 are arbitrary constants that must be determined from the boundary conditions (K_3 is defined by (83)). The boundary conditions on this equation are simply that $\xi = \xi_o$ and that $\dot{\xi} = \dot{\xi}_o$ at $t = 0$. Substituting into Equation 79 and its first derivative yields

$$\xi_o = K_1 + K_2 + K_3 \tag{85}$$

and

$$\dot{\xi} = K_1 m_1 e^{m_1 t} + K_2 m_2 e^{m_2 t} + K_3 ipe^{ipt} \tag{86}$$

$$\dot{\xi}_o = K_1 m_1 + K_2 m_2 + K_3 (ip) \quad . \tag{87}$$

Equations (85) and (87) are easily solved for K_1 and K_2:

$$K_1 = \frac{\dot{\xi}_o - m_2 \xi_o - (ip - m_2) K_3}{m_1 - m_2} \tag{88}$$

$$K_2 = \frac{\dot{\xi}_o - m_1 \xi_o - (ip - m_1) K_3}{m_2 - m_1} \quad . \tag{89}$$

Unfortunately, these deceptively simple equations for K_1 and K_2 are highly complicated, complex variable expressions. To use this solution we have to go back to Equation 73, 74, and 78 and obtain the complete expressions for m_1 and m_2 in aerodynamic terms. They are

$$m_{1,2} = \left[\frac{ipI_x}{2I} + \frac{M_q + M_{\dot{\alpha}}}{2I} \right] \pm \sqrt{\left(- \frac{ipI_x}{2I} - \frac{M_q + M_{\dot{\alpha}}}{2I} \right)^2 + ip \frac{M_{p\beta}}{I} + \frac{M_\alpha}{I}} \quad . \tag{90}$$

Completing the square under the radical,

$$m_{1,2} = \left[\frac{ipI_x}{2I} + \frac{M_q + M_{\dot{\alpha}}}{2I} \right] \pm \sqrt{\left(- \frac{ipI_x}{2I} \right)^2 + 2 \left(\frac{ipI_x}{2I} \right) \left(\frac{M_q + M_{\dot{\alpha}}}{2I} \right) + \left(\frac{M_q + M_{\dot{\alpha}}}{2I} \right)^2 + ip \frac{M_{p\beta}}{I} + \frac{M_\alpha}{I}} \quad . \tag{91}$$

At this point an assumption is made that the term $\left[(M_q + M_{\dot{\alpha}})/(2I) \right]^2$ is small compared to the other terms and may be neglected. This is often true and for many applications it is a legitimate assumption. If this term is deleted and the other terms regrouped the following equation results.

$$m_{1,2} = \left[\frac{ipI_x}{2I} + \frac{M_q + M_{\dot{\alpha}}}{2I} \right] \pm \sqrt{i^2 \left[\left(\frac{pI_x}{2I} \right)^2 - \frac{M_\alpha}{I} \right] + 2 \left(\frac{ipI_x}{2I} \right) \left(\frac{M_q + M_{\dot{\alpha}}}{2I} \right) + ip \frac{M_{p\beta}}{I}} \tag{92}$$

If we let

$$E^2 = i^2 \left[\left(\frac{pI_x}{2I} \right)^2 - \frac{M_\alpha}{I} \right] \tag{93}$$

$$F^2 = 2 \left(\frac{ipI_x}{2I} \right) \left(\frac{M_q + M_{\dot{\alpha}}}{2I} \right) + ip \frac{M_{p\beta}}{I} \tag{94}$$

then

$$m_{1,2} = \left[\frac{ipI_x}{2I} + \frac{M_q + M_{\dot{\alpha}}}{2I}\right] \pm \sqrt{E^2 + F^2} \ , \tag{95}$$

where $\sqrt{E^2 + F^2}$ can be approximated by the binomial expansion

$$\sqrt{E^2 + F^2} = E + \frac{F^2}{2E} - \frac{F^4}{8E^3} + \cdots \tag{96}$$

If $F^2 << E^2$ the series converges rapidly and only the first two terms are required to approximate the radical. Or,

$$\sqrt{E^2 + F^2} \approx E + \frac{F^2}{2E} \ . \tag{97}$$

For most cases this should be an excellent approximation. Substituting (93) and (94) in (97) yields

$$\sqrt{E^2 + F^2} = \pm \left\{ i\sqrt{\left(\frac{pI_x}{2I}\right)^2 - \frac{M_\alpha}{I}} + \frac{\left[2\,\frac{ipI_x}{2I}\left(\frac{M_q + M_{\dot{\alpha}}}{2I}\right)\right] + ip\,\frac{M_{p\beta}}{I}}{2i\sqrt{\left(\frac{pI_x}{2I}\right)^2 - \frac{M_\alpha}{I}}} \right\} . \tag{98}$$

Now from (95)

$$m_{1,2} = \left[\frac{ipI_x}{2I} + \frac{M_q + M_{\dot{\alpha}}}{2I}\right] \pm \left\{ i\sqrt{\left(\frac{pI_x}{2I}\right)^2 - \frac{M_\alpha}{I}} + \frac{\frac{pI_x}{2I}\left(\frac{M_q + M_{\dot{\alpha}}}{2I}\right) + p\,\frac{M_{p\beta}}{2I}}{\sqrt{\left(\frac{pI_x}{2I}\right)^2 - \frac{M_\alpha}{I}}} \right\} . \tag{99}$$

We can now separate real and imaginary parts of $m_{1,2}$ and we let the real part equal $\lambda_{1,2}$ and the imaginary part equal $\omega_{1,2}$.

$$m_{1,2} = \lambda_{1,2} + i\omega_{1,2} = \left[\left(\frac{M_q + M_{\dot{\alpha}}}{2I}\right) \pm \frac{\frac{pI_x}{2I}\left(\frac{M_q + M_{\dot{\alpha}}}{2I}\right) + p\frac{M_{p\beta}}{2I}}{\sqrt{\left(\frac{pI_x}{2I}\right)^2 - \frac{M_\alpha}{I}}}\right] +$$

$$i\left[\left(\frac{pI_x}{2I}\right) \pm \sqrt{\left(\frac{pI_x}{2I}\right)^2 - \frac{M_\alpha}{I}}\right] . \tag{100}$$

Separating this into real and imaginary parts and labeling the real part $\lambda_{1,2}$ (which is often used in connection with damping) and labeling the imaginary part $\omega_{1,2}$ (a symbol normally used for frequency) was not accidental; it required considerable insight. A little rearrangement and algebraic manipulation of (100) provides

$$m_{1,2} = \lambda_{1,2} + i\omega_{1,2} = \left(\frac{M_q + M_{\dot{\alpha}}}{2I}\right)\left[1 \pm \frac{\frac{pI_x}{2I}}{\sqrt{\left(\frac{pI_x}{2I}\right)^2 - \frac{M_\alpha}{I}}}\right] \pm$$

$$\frac{\left(\frac{pI_x}{2I}\right)\left(\frac{M_{p\beta}}{I_x}\right)}{\sqrt{\left(\frac{pI_x}{2I}\right)^2 - \frac{M_\alpha}{I}}} + i\left(\frac{pI_x}{2I}\right)\left[1 \pm \frac{\sqrt{\left(\frac{pI_x}{2I}\right)^2 - \frac{M_\alpha}{I}}}{\frac{pI_x}{2I}}\right] . \tag{101}$$

Now we can let

$$s = \frac{\left(\frac{pI_x}{2I}\right)^2}{\frac{M_\alpha}{I}} , \tag{102}$$

which is called the stability factor. It is a useful expression in determining whether or not a spin stabilized shell will be stable. It must be greater than +1 for gyroscopic stability.

If we define τ as

$$\tau = \frac{1}{\sqrt{1 - \frac{1}{s}}} = \frac{\frac{pI_x}{2I}}{\sqrt{\left(\frac{pI_x}{2I}\right)^2 - \frac{M_\alpha}{I}}} , \tag{103}$$

then Equation 101 becomes

$$m_{1,2} = \lambda_{1,2} + i\omega_{1,2} = \left[\left(\frac{M_q + M_{\dot{\alpha}}}{2I}\right)\left(1 \pm \tau\right) \pm \frac{M_{p\beta}}{I_x}\tau\right] +$$

$$i\left[\frac{pI_x}{2I}\left(1 \pm \frac{1}{\tau}\right)\right] . \tag{104}$$

It should be recognized at this point that τ is really an indicator of the magnitude of the contribution of gyroscopic stability.

Equations 88, 89, 100 and 104 can be used to obtain usable equations for the two constants of integration, K_1 and K_2, in terms of $\lambda_{1,2}$ and $\omega_{1,2}$, which are defined by the aerodynamic coefficients and moments of inertia. Substituting

$$m_{1,2} = \lambda_{1,2} + i\omega_{1,2} ,$$

into Equations 88 and 89 yields

$$K_1 = \frac{\dot{\xi}_o - (\lambda_2 + i\omega_2)\,\xi_o - (ip - \lambda_2 - i\omega_2)\,K_3}{(\lambda_1 + i\omega_1) - (\lambda_2 + i\omega_2)} \tag{106}$$

$$K_2 = \frac{\dot{\xi}_o - (\lambda_1 + i\omega_1)\,\xi_o - (ip - \lambda_1 - i\omega_1)\,K_3}{(\lambda_2 + i\omega_2) - (\lambda_1 + i\omega_1)} . \tag{107}$$

Substituting

$\xi = i\bar{\alpha} + \bar{\beta}$ from Equation 60

$\dot{\xi} = i\dot{\bar{\alpha}} + \dot{\bar{\beta}}$ from Equation 61

$K_3 = iA_3 + B_3$ from Equation 118

and rearranging the denominators of (106) and (107) provides

$$K_1 = \frac{i\dot{\bar{\alpha}}_o + \dot{\bar{\beta}}_o - (\lambda_2 + i\omega_2)\,(i\bar{\alpha}_o + \bar{\beta}_o) - (ip - \lambda_2 - i\omega_2)\,(iA_3 + B_3)}{i\,(\omega_1 - \omega_2) + (\lambda_1 - \lambda_2)} \tag{108}$$

$$K_2 = \frac{i\dot{\bar{\alpha}}_o + \dot{\bar{\beta}}_o - (\lambda_1 + i\omega_1)\,(i\bar{\alpha}_o + \bar{\beta}_o) - (ip - \lambda_1 - i\omega_1)\,(iA_3 + B_3)}{i\,(\omega_2 - \omega_1) + (\lambda_2 - \lambda_1)} . \tag{109}$$

Multiplying and collecting imaginary and real parts

$$K_1 = \frac{i\left[\dot{\bar{\alpha}}_o - \lambda_2\bar{\alpha}_o - \omega_2\bar{\beta}_o + \lambda_2 A_3 - (p - \omega_2)B_3\right]}{i(\omega_1 - \omega_2) + (\lambda_1 - \lambda_2)}$$

$$+\frac{\left[\dot{\bar{\beta}}_o - \lambda_2\bar{\beta}_o + \omega_2\bar{\alpha}_o + (p - \omega_2)A_3 + \lambda_2 B_3\right]}{i(\omega_1 - \omega_2) + (\lambda_1 - \lambda_2)} \tag{110}$$

$$K_2 = \frac{i\left[\dot{\bar{\alpha}}_o - \lambda_1\bar{\alpha}_o - \omega_1\bar{\beta}_o + \lambda_1 A_3 - (p - \omega_1)B_3\right]}{i(\omega_2 - \omega_1) + (\lambda_2 - \lambda_1)}$$

$$+\frac{\left[\dot{\bar{\beta}}_o - \lambda_1\bar{\beta}_o + \omega_1\bar{\alpha}_o + (p - \omega_1)A_3 + \lambda_1 B_3\right]}{i(\omega_2 - \omega_1) + (\lambda_2 - \lambda_1)} \quad . \tag{111}$$

These equations are of the form

$$K = \frac{ia + b}{ic + d} \quad ,$$

and they can be separated into real and imaginary parts by

$$K = \frac{(ia + b)}{(ic + d)}\,\frac{(-ic + d)}{(-ic + d)} = \frac{i(ad - bc) + (ac + bd)}{(c^2 + d^2)} \quad .$$

Consequently,

$$K_1 = i\left[\frac{\left[\dot{\bar{\alpha}}_o - \lambda_2\bar{\alpha}_o - \omega_2\bar{\beta}_o + \lambda_2 A_3 - (p - \omega_2)B_3\right](\lambda_1 - \lambda_2)}{(\omega_1 - \omega_2)^2 + (\lambda_1 - \lambda_2)^2}\right.$$

$$\left. - \frac{\left[\dot{\bar{\beta}}_o - \lambda_2\bar{\beta}_o + \omega_2\bar{\alpha}_o + (p - \omega_2)A_3 + \lambda_2 B_3\right](\omega_1 - \omega_2)}{(\omega_1 - \omega_2)^2 + (\lambda_1 - \lambda_2)^2}\right]$$

$$+\left[\frac{\left[\dot{\bar{\alpha}}_o - \lambda_2\bar{\alpha}_o - \omega_2\bar{\beta}_o + \lambda_2 A_3 - (p - \omega_2)B_3\right](\omega_1 - \omega_2)}{(\omega_1 - \omega_2)^2 + (\lambda_1 - \lambda_2)^2}\right.$$

$$\left. + \frac{\left[\dot{\bar{\beta}}_o - \lambda_2\bar{\beta}_o + \omega_2\bar{\alpha}_o + (p - \omega_2)A_3 + \lambda_2 B_3\right](\lambda_1 - \lambda_2)}{(\omega_1 - \omega_2)^2 + (\lambda_1 - \lambda_2)^2}\right] . \tag{112}$$

$$K_2 = i\left[\frac{\left[\dot{\bar{\alpha}}_o - \lambda_1\bar{\alpha}_o - \omega_1\bar{\beta}_o + \lambda_1 A_3 - (p - \omega_1)B_3\right](\lambda_2 - \lambda_1)}{(\omega_2 - \omega_1)^2 + (\lambda_2 - \lambda_1)^2}\right.$$

$$\left. - \frac{\left[\dot{\bar{\beta}}_o - \lambda_1\bar{\beta}_o + \omega_1\bar{\alpha}_o + (p - \omega_1)A_3 + \lambda_1 B_3\right](\omega_2 - \omega_1)}{(\omega_2 - \omega_1)^2 + (\lambda_2 - \lambda_1)^2}\right]$$

$$+ \left[\frac{\left[\dot{\bar{\alpha}}_o - \lambda_1\bar{\alpha}_o - \omega_1\bar{\beta}_o + \lambda_1 A_3 - (p - \omega_1)B_3\right](\omega_2 - \omega_1)}{(\omega_2 - \omega_1)^2 + (\lambda_2 - \lambda_1)^2}\right.$$

$$\left. + \frac{\left[\dot{\bar{\beta}}_o - \lambda_1\bar{\alpha}_o + \omega_1\bar{\alpha}_o + (p - \omega_1)A_3 + \lambda_1 B_3\right](\lambda_2 - \lambda_1)}{(\omega_2 - \omega_1)^2 + (\lambda_2 - \lambda_1)^2}\right] . \tag{113}$$

A similar procedure is required to separate the real and imaginary parts of K_3. From Equation 83

$$K_3 = \frac{N_3}{(ip - m_1)(ip - m_2)} = \frac{N_3}{(ip - \lambda_1 - i\omega_1)(ip - \lambda_2 - i\omega_2)} . \tag{114}$$

Completing the multiplication and separating the denominator into real and imaginary parts

$$K_3 = \frac{N_3}{i\left[\lambda_2(\omega_1 - p) + \lambda_1(\omega_2 - p)\right] + \left[\omega_2(p - \omega_1) + p(\omega_1 - p) + \lambda_1\lambda_2\right]} . \tag{115}$$

This equation is of the form

$$K_3 = \frac{N_3}{if + g}$$

and can be separated into real and imaginary parts by

$$K_3 = \frac{N_3}{(if + g)}\frac{(-if + g)}{(-if + g)} = \frac{N_3(-if + g)}{(f^2 + g^2)} = \frac{iM_\delta\delta}{I}\left[\frac{-if + g}{f^2 + g^2}\right]$$

$$K_3 = \frac{M_\delta\delta}{I}\left[\frac{ig + f}{f^2 + g^2}\right] .$$

Consequently,

$$K_3 = i\frac{M_\delta \delta}{I}\left[\frac{\omega_2(p-\omega_1)+p(\omega_1-p)+\lambda_1\lambda_2}{\left[\lambda_2(\omega_1-p)+\lambda_1(\omega_2-p)\right]^2+\left[\omega_2(p-\omega_1)+p(\omega_1-p)+\lambda_1\lambda_2\right]^2}\right]$$

$$+\frac{M_\delta \delta}{I}\left[\frac{\lambda_2(\omega_1-p)+\lambda_1(\omega_2-p)}{\left[\lambda_2(\omega_1-p)+\lambda_1(\omega_2-p)\right]^2+\left[\omega_2(p-\omega_1)+p(\omega_1-p)+\lambda_1\lambda_2\right]^2}\right]. \tag{116}$$

Since we now have equations for the three K's in terms of λ and ω, we are ready to break up the exponentials part of the solution into real and imaginary parts. Then it will be possible to obtain real expressions for $\bar{\alpha}$ and $\bar{\beta}$. Recalling Equation 84

$$\xi = K_1 e^{m_1 t} + K_2 e^{m_2 t} + K_3 e^{ipt} ,$$

and since

$$\xi = i\bar{\alpha} + \bar{\beta}$$

$$m_{1,2} = \lambda_{1,2} + i\omega_{1,2}$$

$$i\bar{\alpha} + \bar{\beta} = K_1 e^{(\lambda_1 + i\omega_1)t} + K_2 e^{(\lambda_2 + i\omega_2)t} + K_3 e^{ipt} . \tag{117}$$

Referring to (112), (113) and (116), it can be seen that the K's are complex and are of the form

$$K = iA + B \tag{118}$$

and that the absolute value of K is

$$|K| = \sqrt{A^2 + B^2} .$$

Hence

$$i\bar{\alpha} + \bar{\beta} = (iA_1 + B_1)e^{(\lambda_1 + i\omega_1 t)} + (iA_2 + B_2)e^{(\lambda_2 + i\omega_2)t} + (iA_3 + B_3)e^{ipt} . \tag{119}$$

Now

$$e^{i\omega t} = \cos\omega t + i \sin\omega t .$$

Consequently Equation 119 can be separated into real and imaginary parts by

$$i\bar{\alpha}+\bar{\beta} = e^{\lambda_1 t}\left[i\,(A_1 \cos\omega_1 t + B_1 \sin\omega_1 t) + (B_1 \cos\omega_1 t - A_1 \sin\omega_1 t)\right]$$

$$+ e^{\lambda_2 t}\left[i\,(A_2 \cos\omega_2 t + B_2 \sin\omega_2 t) + (B_2 \cos\omega_2 t - A_2 \sin\omega_2 t)\right]$$

$$+\left[i\,(A_3 \cos pt + B_3 \sin pt) + (B_3 \cos pt - A_3 \sin pt)\right] . \tag{120}$$

Equating $i\bar{\alpha}$ to the imaginary part and $\bar{\beta}$ to the real part of (120) yields the complete expressions for $\bar{\alpha}$ and $\bar{\beta}$, which are

$$\bar{\alpha} = (A_1 \cos\omega_1 t + B_1 \sin\omega_1 t)e^{\lambda_1 t} + (A_2 \cos\omega_2 t + B_2 \sin\omega_2 t)e^{\lambda_2 t}$$

$$+ (A_3 \cos pt + B_3 \sin pt) \tag{121}$$

$$\bar{\beta} = (B_1 \cos\omega_1 t - A_1 \sin\omega_1 t)e^{\lambda_1 t} + (B_2 \cos\omega_2 t - A_2 \sin\omega_2 t)e^{\lambda_2 t}$$

$$+ (B_3 \cos pt - A_3 \sin pt) , \tag{122}$$

where the A's and B's are obtained from (112), (113), (116), and (118). They are

$$A_1 = \left[\frac{\left[\dot{\bar{\alpha}}_o - \lambda_2\bar{\alpha}_o - \omega_2\bar{\beta}_o + \lambda_2 A_3 - (p - \omega_2)\,B_3\right](\lambda_1 - \lambda_2)}{(\omega_1 - \omega_2)^2 + (\lambda_1 - \lambda_2)^2}\right.$$

$$\left. - \frac{\left[\dot{\bar{\beta}}_o - \lambda_2\bar{\beta}_o + \omega_2\bar{\alpha}_o + (p - \omega_2)\,A_3 + \lambda_2 B_3\right](\omega_1 - \omega_2)}{(\omega_1 - \omega_2)^2 + (\lambda_1 - \lambda_2)^2}\right] \tag{123}$$

$$B_1 = \left[\frac{\left[\dot{\bar{\alpha}}_o - \lambda_2\bar{\alpha}_o - \omega_2\bar{\beta}_o + \lambda_2 A_3 - (p - \omega_2)\,B_3\right](\omega_1 - \omega_2)}{(\omega_1 - \omega_2)^2 + (\lambda_1 - \lambda_2)^2}\right.$$

$$\left. + \frac{\left[\dot{\bar{\beta}}_o - \lambda_2\bar{\beta}_o + \omega_2\bar{\alpha}_o + (p - \omega_2)\,A_3 + \lambda_2 B_3\right](\lambda_1 - \lambda_2)}{(\omega_1 - \omega_2)^2 + (\lambda_1 - \lambda_2)^2}\right] \tag{124}$$

$$A_2 = \left[\frac{\left[\dot{\bar{\alpha}}_o - \lambda_1 \bar{\alpha}_o - \omega_1 \bar{\beta}_o + \lambda_1 A_3 - (p - \omega_1) B_3\right] (\lambda_2 - \lambda_1)}{(\omega_2 - \omega_1)^2 + (\lambda_2 - \lambda_1)^2} \right.$$

$$\left. - \frac{\left[\dot{\bar{\beta}}_o - \lambda_1 \bar{\beta}_o + \omega_1 \bar{\alpha}_o + (p - \omega_1) A_3 + \lambda_1 B_3\right] (\omega_2 - \omega_1)}{(\omega_2 - \omega_1)^2 + (\lambda_2 - \lambda_1)^2} \right] \tag{125}$$

$$B_2 = \left[\frac{\left[\dot{\bar{\alpha}}_o - \lambda_1 \bar{\alpha}_o - \omega_1 \bar{\beta}_o + \lambda_1 A_3 - (p - \omega_1) B_3\right] (\omega_2 - \omega_1)}{(\omega_2 - \omega_1)^2 + (\lambda_2 - \lambda_1)^2} \right.$$

$$\left. + \frac{\left[\dot{\bar{\beta}}_o - \lambda_1 \bar{\beta}_o + \omega_1 \bar{\alpha}_o + (p - \omega_1) A_3 + \lambda_1 B_3\right] (\lambda_2 - \lambda_1)}{(\omega_2 - \omega_1)^2 + (\lambda_2 - \lambda_1)^2} \right] \tag{126}$$

$$A_3 = \frac{M_\delta \delta}{I} \left[\frac{\omega_2 (p - \omega_1) + p (\omega_1 - p) + \lambda_1 \lambda_2}{\left[\lambda_2 (\omega_1 - p) + \lambda_1 (\omega_2 - p)\right]^2 + \left[\omega_2 (p - \omega_1) + p (\omega_1 - p) + \lambda_1 \lambda_2\right]^2} \right] \tag{127}$$

$$B_3 = \frac{M_\delta \delta}{I} \left[\frac{\lambda_2 (\omega_1 - p) + \lambda_1 (\omega_2 - p)}{\left[\lambda_2 (\omega_1 - p) + \lambda_1 (\omega_2 - p)\right]^2 + \left[\omega_2 (p - \omega_1) + p (\omega_1 - p) + \lambda_1 \lambda_2\right]^2} \right] , \tag{128}$$

where $\bar{\alpha}_o$, $\dot{\bar{\alpha}}_o$, $\bar{\beta}_o$ and $\dot{\bar{\beta}}_o$ are the initial angle and angular rate conditions, and $\lambda_{1,2}$ and $\omega_{1,2}$ (which have been defined in Equations 101 and 104) are

$$\lambda_{1,2} = \left(\frac{M_q + M_{\dot{\alpha}}}{2I}\right)(1 \pm \tau) \pm \frac{M_{p\beta}}{I_x} \tau = \left(\frac{M_q + M_{\dot{\alpha}}}{2I}\right)\left[1 \pm \frac{\frac{pI_x}{2I}}{\sqrt{\left(\frac{pI_x}{2I}\right)^2 - \frac{M_\alpha}{I}}}\right] \pm \tag{129}$$

$$\frac{\left(\frac{pI_x}{2I}\right)\left(\frac{M_{p\beta}}{2I_x}\right)}{\sqrt{\left(\frac{pI_x}{2I}\right)^2 - \frac{M_\alpha}{I}}}$$

$$\omega_{1,2} = \left(\frac{pI_x}{2I}\right)\left(1 \pm \frac{1}{\tau}\right) = \frac{pI_x}{2I} \pm \sqrt{\left(\frac{pI_x}{2I}\right)^2 - \frac{M_\alpha}{I}} , \tag{130}$$

where the subscript 1 refers to the + signs and the subscript 2 to the - signs. The equations for $\bar{\alpha}$ and $\bar{\beta}$ are obviously complicated and require the computation of ten constants before $\bar{\alpha}$ and $\bar{\beta}$ can be calculated as a function of time. Fortunately they can be simplified to some extent for many applications, which are considered in the next section.

Application

Assuming that the problem meets the linearity and small angle restrictions, that the physical and aerodynamic characteristics are known, and that the initial angle conditions are known, the motion of a vehicle can be calculated directly from the complete Equations 121 through 130. These equations are complicated and would normally require machine computation. Fortunately it is possible to greatly simplify the equations for most applications.

Simplified Equations

The basic Equations 121 and 122 for $\bar{\alpha}$ and $\bar{\beta}$ cannot be simplified; however, most of the complication is in the expressions for the A's and B's, which can be simplified. In many flight systems the static stability is much greater than the dynamic stability, so that $\lambda_{1,2} \ll \omega_{1,2}$. This is usually, but not always, true for fin stabilized rockets and bombs, and is often true for re-entry vehicles. This condition provides the basis for eliminating all terms involving $\lambda_{1,2}$ in the equations for A and B:

$$A_1 = -\left[\frac{\dot{\bar{\beta}}_o + \omega_2 \bar{\alpha}_o + (p - \omega_2) A_3}{\omega_1 - \omega_2}\right] \tag{131}$$

$$B_1 = \left[\frac{\dot{\bar{\alpha}}_o - \omega_2 \bar{\beta}_o}{\omega_1 - \omega_2}\right] \tag{132}$$

$$A_2 = -\left[\frac{\dot{\bar{\beta}}_o + \omega_1 \alpha_o + (p - \omega_1) A_3}{\omega_2 - \omega_1}\right] \tag{133}$$

$$B_2 = \left[\frac{\dot{\bar{\alpha}}_o - \omega_1 \bar{\beta}_o}{\omega_2 - \omega_1}\right] \tag{134}$$

$$A_3 = \frac{M_\delta \delta}{I}\left[\frac{1}{\omega_2 (p - \omega_1) + p (\omega_1 - p)}\right], \quad (p \neq \omega_1) \tag{135}$$

$$B_3 = 0, \quad (p \neq \omega_1). \tag{136}$$

The percentage error involved in this simplification is approximately $\sqrt{2}\,(\lambda_{1,2}/\omega_{1,2})\,100\%$. For two-arm or epicyclic motion (zero trim), the equations for the A's and B's reduce further to

$$A_1 = -\left[\frac{\dot{\bar{\beta}}_o + \omega_2 \bar{\alpha}_o}{\omega_1 - \omega_2}\right] \tag{137}$$

$$B_1 = \left[\frac{\dot{\bar{\alpha}}_o - \omega_2 \bar{\beta}_o}{\omega_1 - \omega_2}\right] \tag{138}$$

$$A_2 = -\left[\frac{\dot{\bar{\beta}}_o + \omega_1 \bar{\alpha}_o}{\omega_2 - \omega_1}\right] \tag{139}$$

$$B_2 = \left[\frac{\dot{\bar{\alpha}}_o - \omega_1 \bar{\beta}_o}{\omega_2 - \omega_1}\right] \tag{140}$$

$$A_3 = B_3 = 0 \ . \tag{150}$$

Example Problem

To demonstrate the accuracy of the simplified approach, two sample problems were calculated using the Tricyclic Theory and a Six-Degree-of-Freedom computer program,[7] and the results were compared. The example was deliberately chosen to be as linear as possible, yet it is representative of a supersonic fin stabilized rocket. The rocket was launched at an angle of 1° above the horizontal and zero drag was assumed to maintain a constant dynamic pressure. The vehicle characteristics are listed in Table I. The static moment derivative is calculated from Equation 48:

$$M_\alpha = C_{m\alpha}\, q'\, Sd$$

$$M_\alpha = -30\ (400.35)\ (0.442)\ (.75) = -3982 \ .$$

The frequencies are obtained from Equation 130:

$$\omega_{1,2} = \left(\frac{pI_x}{2I}\right) \pm \sqrt{\left(\frac{pI_x}{2I}\right)^2 - \frac{M_\alpha}{I}}$$

$$\omega_{1,2} = \left(\frac{37.7\ (3.37)}{2\ (101)}\right) \pm \left[\left(\frac{37.3\ (3.37)}{2\ (101)}\right)^2 - \frac{-3982}{101}\right]^{1/2}$$

$$\omega_{1,2} = 0.629 \pm 6.307 = +\ 6.936,\ -\ 5.678 \text{ rad/sec} \ .$$

TABLE I

Vehicle Characteristics and Flight Conditions
(Sample Problem)

q'	= 400.35 psf
I_x	= 3.37 slug-ft^2
I	= 101 slug-ft^2
S	= 0.442 ft^2
d	= 0.75 ft
p	= 37.7 rad per sec
$C_{m\alpha}$	= -30 per radian
$C_{mq} + C_{m\dot{\alpha}}$	= -1400 per rad/sec
$C_{m\delta}$	= +30 per radian
δ	= 2 degrees

The damping moment derivative is calculated from Equations 50 and 52:

$$M_q + M_{\dot{\alpha}} = (C_{mq} + C_{m\dot{\alpha}}) \frac{q' Sd^2}{2V}$$

$$M_q + M_{\dot{\alpha}} = \frac{(-1400)\,(400.35)\,(0.442)\,(0.75)^2}{2\,(5000)}$$

$$M_q + M_{\dot{\alpha}} = -13.93 \text{ ft-pounds/rad per sec}$$

The λ's are obtained from Equation 129:

$$\lambda_{1,2} = \frac{M_q + M_{\dot{\alpha}}}{2I}\,(1 \pm \tau)$$

$$\lambda_{1,2} = \frac{-13.93}{2\,(101)}\,(1 \pm 0.0997) = -0.0758,\ -0.0621\ ,$$

where τ is

$$\tau = \frac{\dfrac{pI_x}{2I}}{\sqrt{\left(\dfrac{pI_x}{2I}\right)^2 - \dfrac{M_\alpha}{I}}} = \frac{0.629}{6.307} = 0.0997\ .$$

Both example problems are identical, except that the first calculation has a trim angle ($\delta = +2^\circ$) and is tricyclic (all three arms are present) and in the second example the motion is epicyclic.

The initial conditions are the same for both examples, that is,

$$\bar{\alpha}_o = 10^o$$

$$\dot{\bar{\alpha}}_o = 0$$

$$\bar{\beta}_o = 0$$

$$\dot{\bar{\beta}}_o = 0 \ .$$

The A's and B's are computed from Equations 131 through 136.

<u>Tricyclic Case</u>

$$A_3 = \frac{M_\delta \delta}{I} \left[\frac{1}{\omega_2 (p - \omega_1) + p (\omega_1 - p)} \right]$$

$$A_3 = \frac{3982}{101} (2) \left[\frac{1}{(-5.678)(37.7 - 6.936) + (37.7)(6.936 - 37.7)} \right]$$

$$A_3 = -0.0591^o$$

$$B_3 = 0$$

$$A_1 = - \left[\frac{\dot{\bar{\beta}}_o + \omega_2 \bar{\alpha}_o + (p - \omega_2) A_3}{\omega_1 - \omega_2} \right]$$

$$A_1 = - \left[\frac{0 + (-5.678)(10) + [37.7 - (5.678)](-0.0591)}{6.396 - (-5.678)} \right]$$

$$A_1 = +4.705^o$$

$$B_1 = \left[\frac{\dot{\bar{\alpha}}_o - \omega_2 \bar{\beta}_o}{\omega_1 - \omega_2} \right] = \left[\frac{0 - (-5.678)(0)}{6.936 - (-5.678)} \right] = 0$$

$$A_2 = - \left[\frac{\dot{\bar{\beta}}_o + \omega_1 \bar{\alpha}_o + (p - \omega_1) A_3}{\omega_2 - \omega_1} \right]$$

$$A_2 = -\left[\frac{0 + 6.936\,(10) + (37.7 - 6.936)\,(-0.0591)}{-5.678 - 6.936}\right] = +5.354$$

$$B_2 = \left[\frac{\dot{\bar{\alpha}}_o - \omega_1\bar{\beta}_o}{\omega_2 - \omega_1}\right] = \left[\frac{0 - 6.936\,(0)}{-5.678 - 6.936}\right] = 0 \ .$$

Since

$$|K| = \sqrt{A^2 + B^2}$$

$$|K_1| = 4.705^o$$

$$|K_2| = 5.354^o$$

$$|K_3| = 0.0591^o$$

<u>Epicyclic Case</u>

$$A_1 = -\left[\frac{\dot{\bar{\beta}}_o + \omega_2\bar{\alpha}_o}{\omega_1 - \omega_2}\right] = -\left[\frac{0 + (-5.678)\,10}{6.936 - (-5.678)}\right] = +4.501^o$$

$$B_1 = \left[\frac{\dot{\bar{\alpha}}_o - \omega_2\bar{\beta}_o}{\omega_1 - \omega_2}\right] = 0$$

$$A_2 = -\left[\frac{\dot{\bar{\beta}}_o + \omega_1\bar{\alpha}_o}{\omega_2 - \omega_1}\right] = -\left[\frac{0 + (6.936)\,10}{-5.678 - 6.936}\right] = +5.499^o$$

$$A_3 = B_3 = 0$$

$$|K_1| = 4.501^o$$

$$|K_2| = 5.499^o$$

$$|K_3| = 0 \ .$$

Note that rather small K_3 arm (0.059^o) has a large effect on the size of the K_1 and K_2 arms, which causes a much larger effect on the motion than might be expected, and usually should not be ignored. Also notice that initially both the K_1 and K_2 arms are pointed upward along the

$+\tilde{\alpha}$ axis and the K_3 arm is pointed downward along the $\tilde{\alpha}$ axis.* The calculations for both the tricyclic and epicyclic examples are shown in Appendix A and are plotted on Figures 5 and 6 in comparison with the 6 DOF computer calculation. The agreement is excellent, as can be seen on the plots and by comparing columns 21 and 22 with columns 23 and 24 in Appendix A for the tricyclic example and comparing columns 31 and 32 with columns 33 and 34 for the epicyclic case.

The error is approximately 1.5%, which is sufficiently accurate for most flight dynamics purposes.

Discussion

The Tricyclic Theory is the only existing theory that is capable of predicting the motion of a flight vehicle in considerable detail by means of a closed form solution. Other flight dynamics techniques involve the numerical integration of the equations of motion. The most complete form of numerical integration, the 6 DOF computer codes, provide complete nonlinear and time variant solutions; however, it is often difficult to obtain a thorough understanding of the motion required to diagnose flight dynamics problems. Conversely, the Tricyclic Theory provides the basic underlying principles of the motion but is restricted in application to linear or quasi-linear and time invariant or quasi-time invariant problems. For these reasons it is important that the Tricyclic Theory be applied to flight dynamics problems and that its restrictions be understood.

Constant Coefficient Restriction

Constant coefficients (N_1, N_2 and N_3) are assumed in solving Equation 76. Unfortunately, this occurs in few flight dynamics problems, because M_α and $(M_q + M_{\dot{\alpha}})$ almost always vary with time and often change with angle of attack (nonlinear). Aeroelasticity is an often overlooked but serious contributor to nonlinearity. To further complicate the situation, there are no simple established specifications on the error involved in applying the theory to problems where the coefficients vary with time or are nonlinear. However, two comments can be made in this regard. First, a nonconstant coefficient problem can often be reduced to a quasi-constant coefficient problem by dividing the problem into small time increments, so that the coefficients do not change significantly during the time increments. Second, $\omega_{1,2}$ appears to have the largest effect on the magnitude of K_1 and K_2; consequently, variations in M_α probably cause the largest nonlinear effects. While indiscriminate application of this theory is inadvisable, application with caution can often solve a flight dynamics problem that otherwise would not be possible to solve.

*In the 6 DOF Aeroballistic System. See section entitled Physical Interpretation.

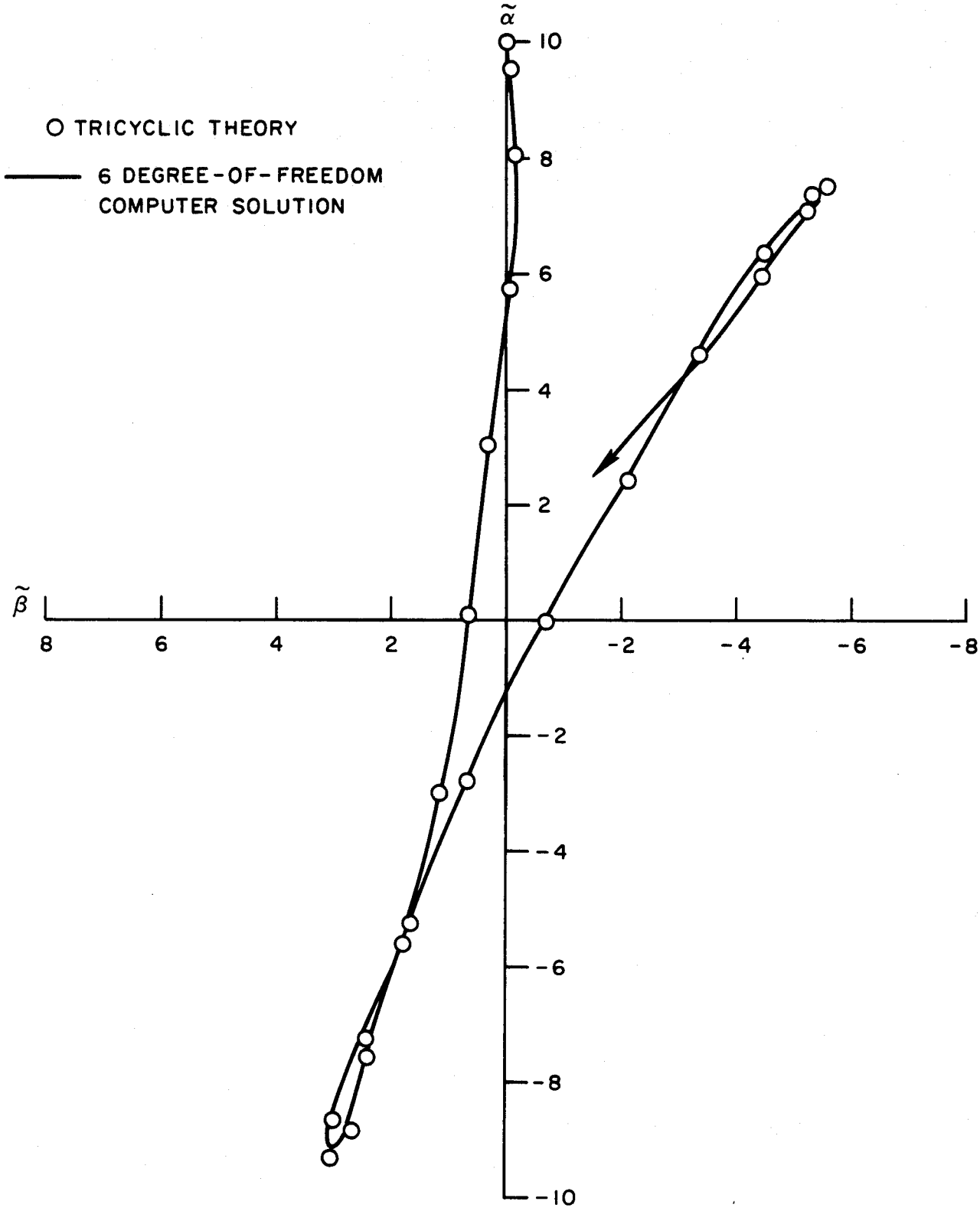

Figure 5. Comparison of Tricyclic Theory with 6 DOF Calculation

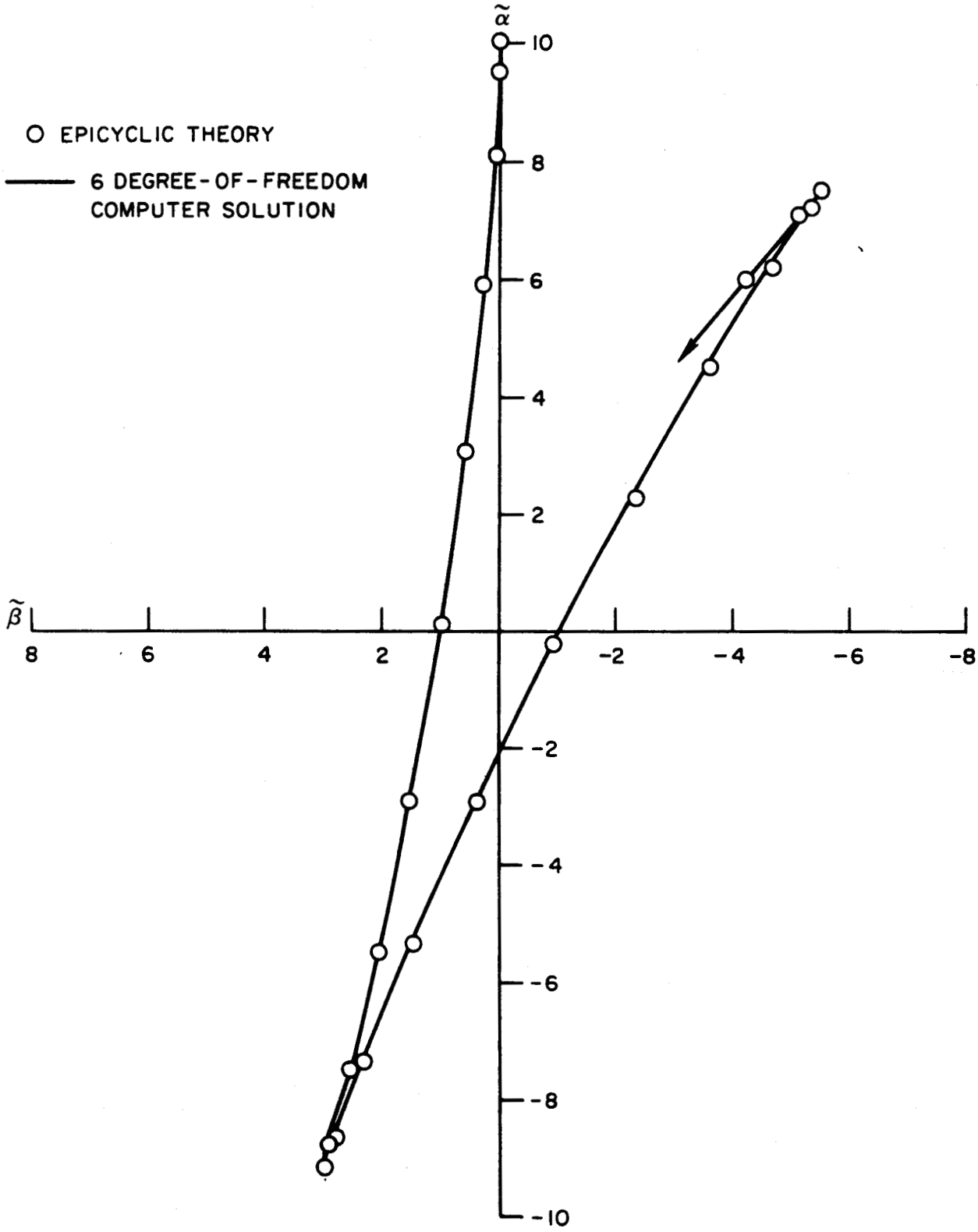

Figure 6. Comparison of Epicyclic Theory with 6 DOF Calculation

Small Angle Restriction

Inherent in the definition of the applied aerodynamic moments in the aeroballistic equations is a small angle of attack restriction that is not immediately apparent. This results because the total velocity vector (V) cannot remain perpendicular to both the $\bar{y}$ and $\bar{z}$ axes when both $\bar{\alpha}$ and $\bar{\beta}$ are present. The distortion in the angles is demonstrated in Figure 7, where both $\bar{y}$ and $\bar{z}$ have been rotated so that $|\xi| \cong 90^{\circ}$ and $\bar{\alpha} = \bar{\beta}$. It can be shown from trigonometry that

$$\bar{\alpha}_1 = \bar{\alpha}_2 = \bar{\beta}_1 = \bar{\beta}_2 \cong 45^{\circ}$$

$$\bar{\alpha} = \bar{\beta} \cong 60^{\circ} \ .$$

From this geometry it is possible to see that the true angle of attack and the sideslip $(\bar{\alpha}_t, \bar{\beta}_t)$ that would normally be associated with the aerodynamic coefficients are

$$\bar{\alpha}_t = \bar{\alpha} \cos \bar{\beta}$$

$$\bar{\beta}_t = \bar{\beta} \cos \bar{\alpha} \ .$$

The error caused by this assumption can be approximated as follows for circular coning motion. The frequency ω_1 is approximately

$$\omega_1 \cong \sqrt{\frac{M_\alpha}{I}} \ ,$$

so that the error in ω_1 is approximately

$$\Delta\omega_1 \cong \sqrt{\frac{M_\alpha}{I} \left(\frac{\bar{\alpha}}{\bar{\alpha} \cos \bar{\beta}}\right)} \ ,$$

which for a 10° total angle of attack is

$$\Delta\omega_1 = \omega_1 \sqrt{\frac{1}{\cos 10^{\circ}}} = \frac{\omega_1}{.99237} \ .$$

Or, the maximum error in frequency would be 0.76% and the average error would be roughly 0.48%. Therefore this restriction is not too significant as long as the angles are small.

Physical Interpretation

A physical interpretation of the Tricyclic solution is somewhat complicated by the complex algebra that is involved. An attempt is made in Figure 8 to provide a graphical description of the solution. The first thing to be recognized is that the equations of motion that are solved

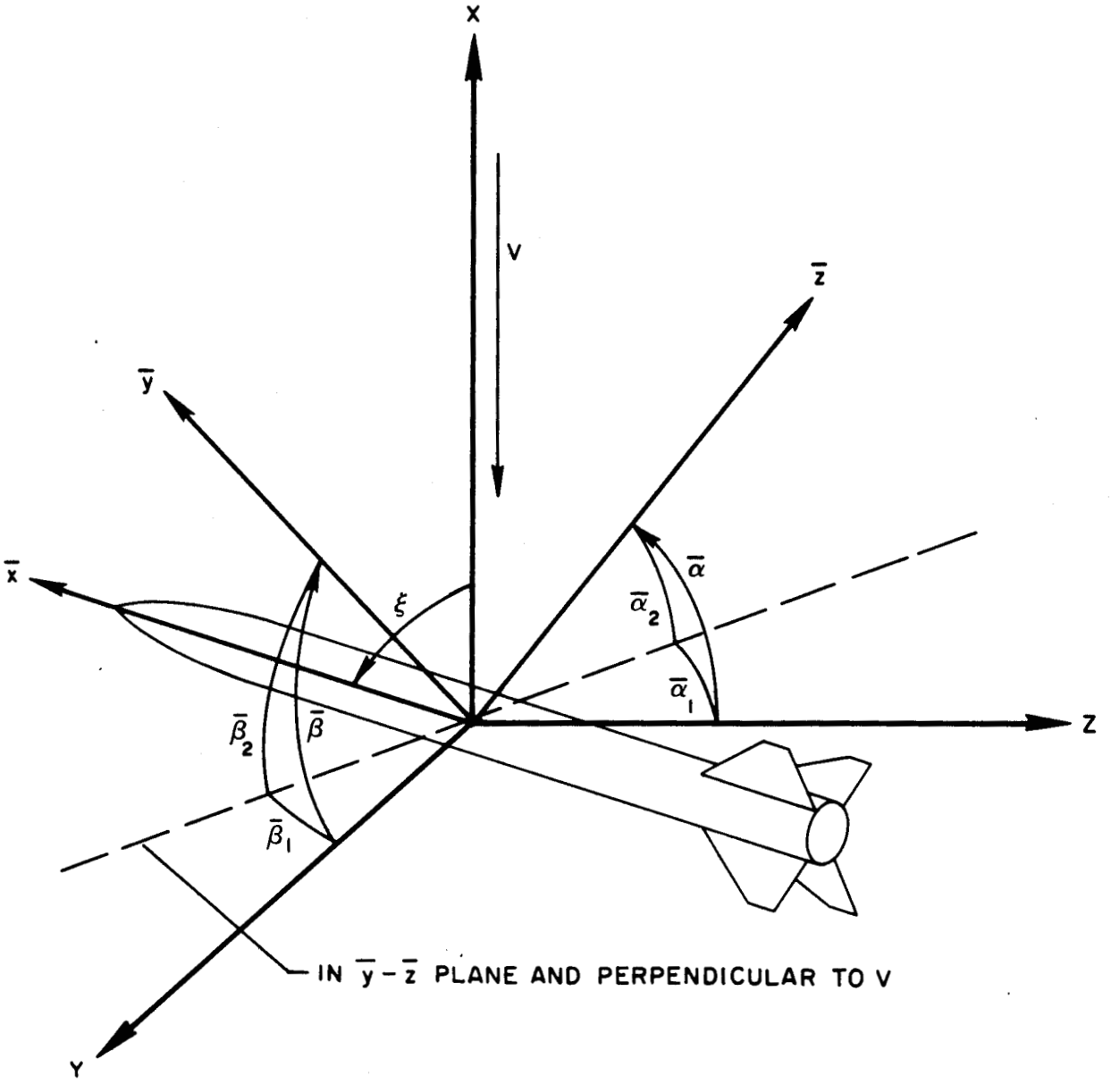

Figure 7. Effect of Large Angle on $\bar{\alpha}$ and $\bar{\beta}$

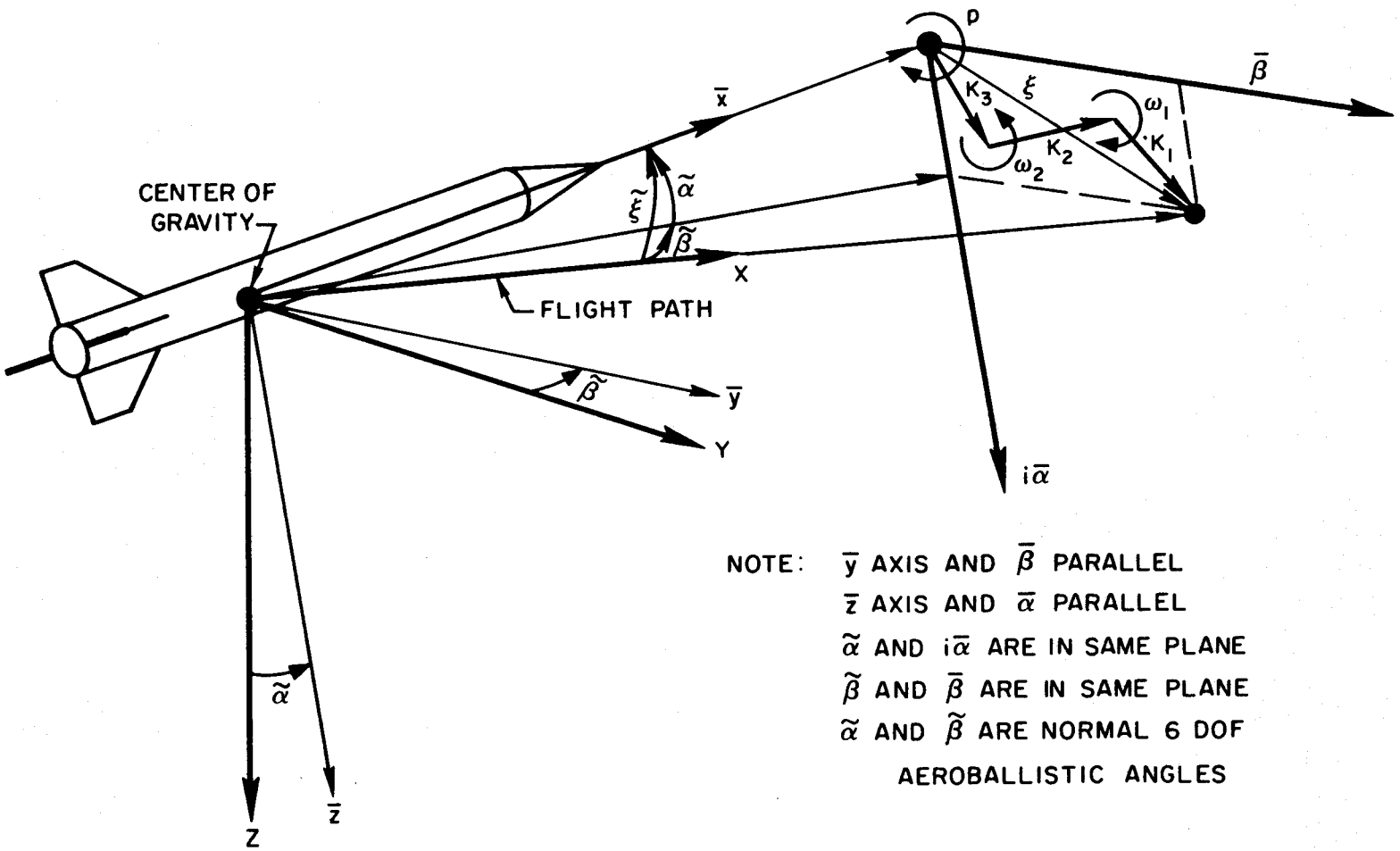

Figure 8. Physical Interpretation of Tricyclic Theory

constitute the sums of the moments about the body $\bar{y}$ and $\bar{z}$ axes. Consequently, ω_1 and ω_2 must be about the body axes. The solution, repeated below from Equation 84, indicates that ω_1, ω_2, and p must all be about the same axis.

$$\xi = K_1 e^{(\lambda_1 + i\omega_1)t} + K_2 e^{(\lambda_2 + i\omega_2)t} + K_3 e^{ipt} ,$$

and since p is about the body $\bar{x}$ axis, ω_1 and ω_2 must also be about the $\bar{x}$ axis. Consequently, the three K's rotate about the $\bar{x}$ axis at their respective frequencies and describe the motion of the flight path with respect to the body $\bar{x}$ axis. This is opposite to the normal convention used in the aeroballistic option of 6 DOF programs. However, the whole thing can be inverted without any sign reversals resulting ($i\bar{\alpha}$ and $\bar{\beta}$ are interchangeable with $\tilde{\alpha}$ and $\tilde{\beta}$). This is shown in an $\tilde{\alpha}$-$\tilde{\beta}$ plot in Figure 9, where $\tilde{\alpha}$ and $\tilde{\beta}$ are the aeroballistic angles measured from the flight path to the body $\bar{x}$ axis. It should be noted from the solution that the order of addition of the K's is unimportant and consequently the order of the K arms in Figure 9 is unimportant. Equation 119 shows the complete solution where the K's are shown in complex form:

$$i\bar{\alpha} + \bar{\beta} = (iA_1 + B_1)\, e^{(\lambda_1 + i\omega_1)t} + (iA_2 + B_2)\, e^{(\lambda_2 + i\omega_2)t} + (iA_3 + B_3)\, e^{ipt} .$$

If we let t = o in this equation,

$$i\bar{\alpha}_o + \bar{\beta}_o = (iA_1 + B_1) + (iA_2 + B_2) + (iA_3 + B_3)$$

and

$$\bar{\alpha}_o = A_1 + A_2 + A_3$$

$$\bar{\beta}_o = B_1 + B_2 + B_3 .$$

Therefore, the A's and B's are simply the $\bar{\alpha}$ and $\bar{\beta}$ components under initial conditions. It also follows that the ψ angles shown in Figure 9 can be calculated from

$$\psi_1 = \tan^{-1} \frac{B_1}{A_1} + \omega_1 t$$

and similarly for ψ_2 and ψ_3.

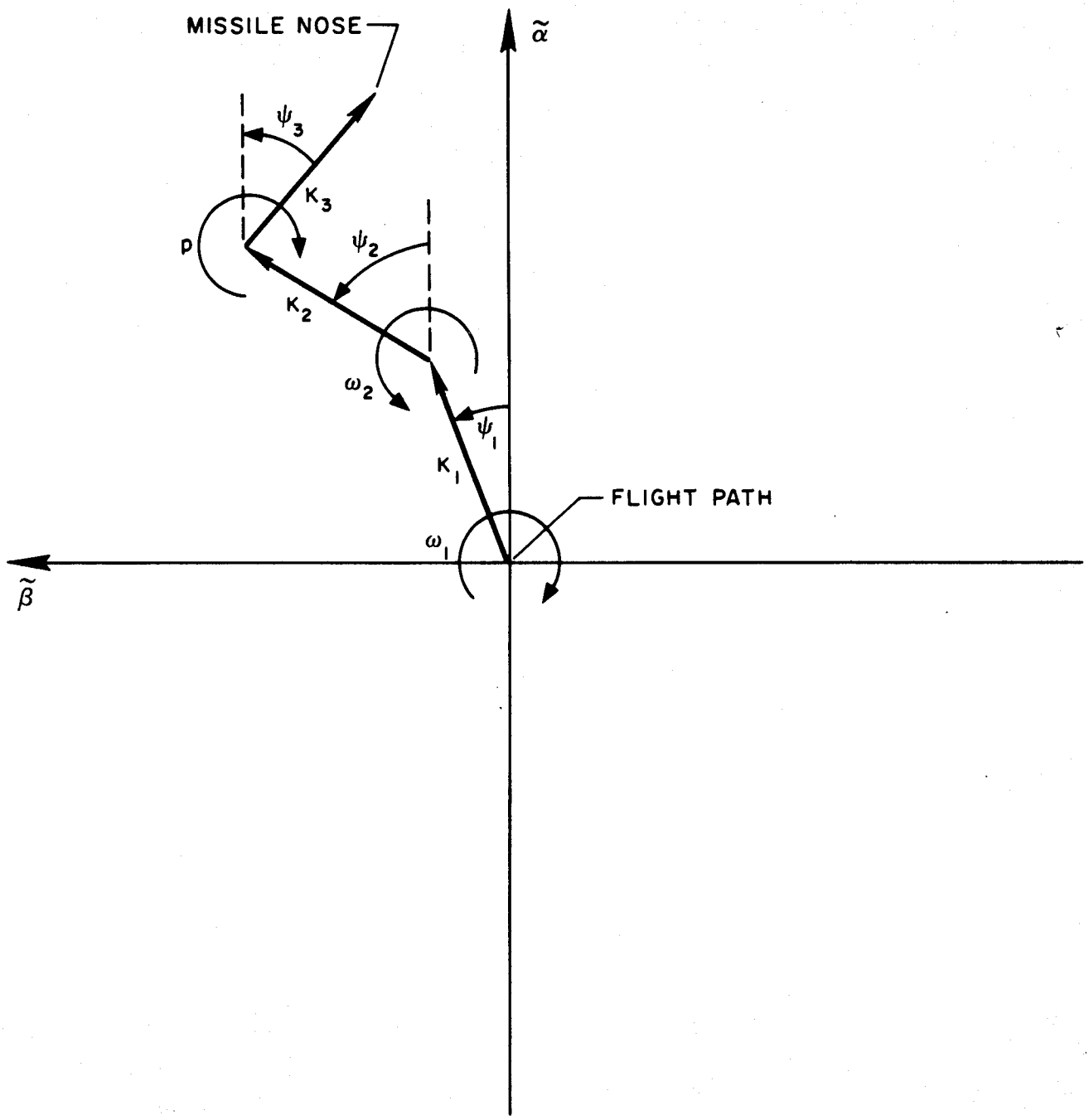

Figure 9. $\tilde{\alpha}$ - $\tilde{\beta}$ Plot

The three K's or arms and the three associated frequencies have been previously defined as follows:

K_1 - nutation arm	ω_1 - nutation frequency (high frequency)
K_2 - precession arm	ω_2 - precession frequency (low frequency)
K_3 - trim arm	p - roll frequency

While these particular definitions may be in conflict with gyroscopic terminology it is important that they be maintained; otherwise confusion may result. The fact that the nutation arm (K_1) <u>always</u> rotates in the same direction as the roll rate (p) and that the precession arm (K_2) <u>always</u> rotates opposite to p, for an aerodynamically statically stable body is important. This is easily seen from Equation 130, which is repeated below.

$$\omega_{1,2} = p\frac{I_x}{2I} \pm \sqrt{\left(p\frac{I_x}{2I}\right)^2 - \frac{M_\alpha}{I}} \ .$$

For a statically stable body $\frac{M_\alpha}{I}$ is always negative; consequently the radical is always greater than $(p\,I_x)/(2I)$, and ω_1 will be positive and ω_2 negative for a positive p. Also if M_α/I is small (corresponding to exoatmospheric flight), $\omega_{1,2}$ become one frequency

$$\left(\omega_1 = p\frac{I_x}{I}\right) ,$$

which is the gyroscopic frequency. Conversely, if $M\alpha/I$ is large compared to $(pI_x)/(2I)$, which corresponds to normal aerodynamically stable flight at high dynamic pressures, then

$$\omega_1 \cong \sqrt{\frac{-M_\alpha}{I}} ,$$

which is a well known approximation of the nutation frequency. The gyroscopic frequency is usually 5 to 10% of the aerodynamic frequency on a fin stabilized rocket vehicle flying at high dynamic pressure.

Characteristic Motion

While an infinite variety of motion patterns can be generated by the Tricyclic Theory, a few types tend to predominate. Some of these have been generated by a mechanical device to illustrate epicyclical motion.

The motion shown in Figure 10 is for the case of zero roll rate (p = 0) when the nutation and precession frequencies are equal ($\omega_1 = \omega_2$). Figure 10 shows the characteristic types of motion with different initial conditions. In Figure 10 (a) planar motion is generated when K_1 and K_2 are equal, which is the case when $\dot{\beta}_o$ is zero. As a progressively larger negative value of

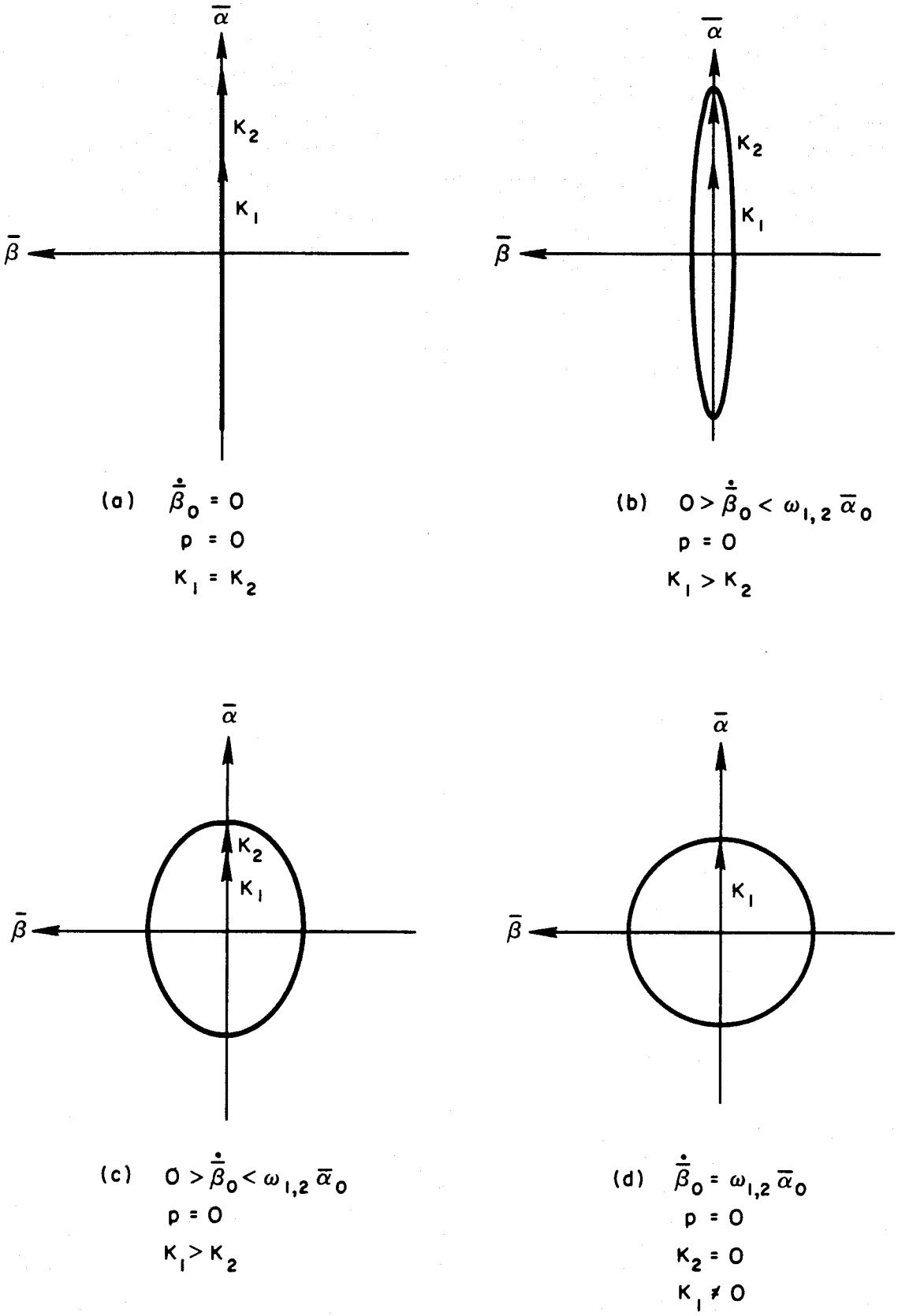

Figure 10. Characteristic Motion with Zero Roll Rate

$\dot{\bar{\beta}}_o$ is introduced, the K_2 arm will reduce (see Equations 137 through 140) and K_1 is maintained the same length, resulting in an elliptical motion (Figures 10 (b) and 10 (c)). Finally as $\dot{\bar{\beta}}_o$ becomes equal to $\omega_{1,2}\bar{\alpha}_o$, the K_2 arm becomes zero and circular motion results with only the K_1 arm remaining. If the negative value for $\dot{\bar{\beta}}_o$ is increased further so that it is greater than $\omega_{1,2}\bar{\alpha}_o$, elliptical motion results with the major axis being along the $\bar{\beta}$ axis. In this set of sketches K_1 is kept constant, and $\bar{\alpha}_o$ varies and is simply equal to the sum of K_1 and K_2. This condition is inherent in the mechanical device used to generate the sketches.

Figure 11 is a similar set of motion patterns for a rolling vehicle. In this case the nutation frequency is greater than the precessional frequency ($\omega_1 = -1.083\,\omega_2$), which is typical of fin stabilized vehicles. The unequal frequencies cause the oscillatory plane to rotate in the direction of ω_1 and p, since ω_1 is larger than ω_2. The angular rate of this precessing motion ($\dot{\psi}_o$) is

$$\Delta\psi_o = \omega_1\Delta t + \omega_2\Delta t$$

$$\dot{\psi}_o = \frac{\Delta\psi_o}{\Delta t} = \omega_1 + \omega_2 = \frac{pI_x}{I} .$$

Consequently the magnitude of $\dot{\psi}_o$ depends only on the roll rate and moment of inertia ratio of the vehicle. Also, it can be shown that ψ_o depends only on ω_1/ω_2:

$$\psi_o = \frac{2\pi\left(\frac{\omega_1}{\omega_2} + 1\right)}{\left(\frac{\omega_1}{\omega_2} - 1\right)}$$

Figure 11 (a) demonstrates a pointed cusp pattern that results from $\dot{\bar{\beta}}_o$ being zero. As $\dot{\bar{\beta}}_o$ increases in a negative direction, the loops are formed which change into ellipses in Figures 11 (c) and (d). As before, K_1 is constant and K_2 gradually decreases as $\dot{\bar{\beta}}_o$ is increased in a negative direction. This reduction of K_2 with respect to K_1 as $-\dot{\bar{\beta}}_o$ is increased can be seen in Equations 137 and 139.

Aerodynamic damping was ignored in generating the motion patterns. Normally, damping would gradually decrease the magnitude of K_1 and K_2 if the vehicle is dynamically stable.

Magnus Moment

The magnus moment, which results from combined angle of attack and roll rate, was included in the theory, since it can be important when the body is rolling at a high frequency. Magnus moment is usually important on a spin stabilized shell and is normally considered unimportant on a fin stabilized vehicle. This can be qualitatively demonstrated by examining the $\lambda_{1,2}$ equation for a 6-inch-diameter spin stabilized shell and a high fineness ratio fin stabilized rocket.

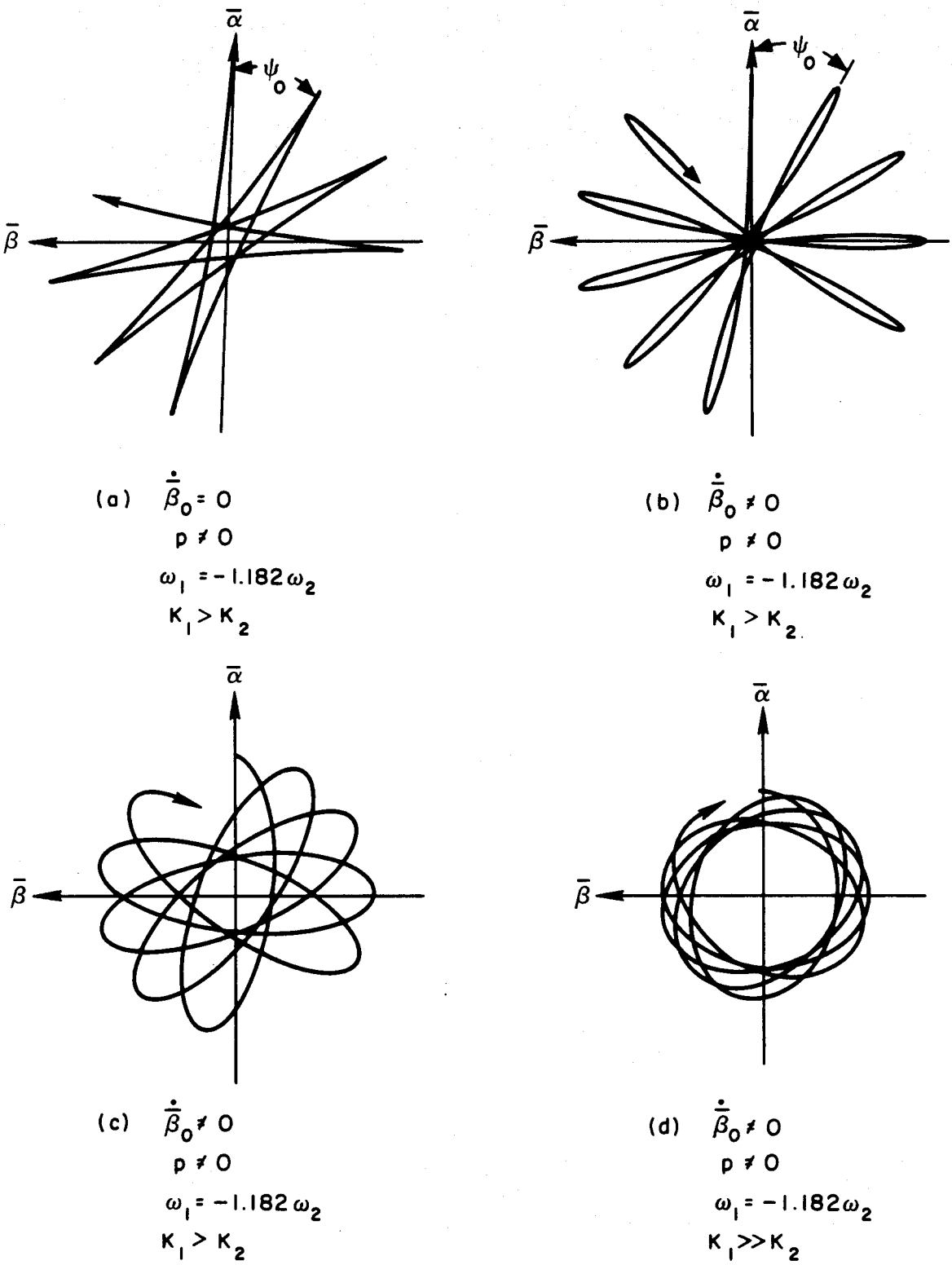

Figure 11. Characteristic Motion of Rolling Body

For a typical 6-inch spin stabilized shell, τ is approximately 2; therefore from Equation 129:

$$\lambda_{1,2} = \left(\frac{M_q + M_{\dot{\alpha}}}{2I}\right)(1 \pm \tau) \pm \frac{M_{p\beta}}{I_x}(\tau)$$

$$\lambda_{1,2} = \left(\frac{M_q + M_{\dot{\alpha}}}{2I}\right)(1 \pm 2) \pm \frac{M_{p\beta}}{I_x}(2) \ .$$

Now I_x is about 0.1 and I about 1.5 for the shell.

$$\lambda_{1,2} = (M_q + M_{\dot{\alpha}})\left(\frac{1 \pm 2}{3}\right) \pm M_{p\beta}\left(\frac{2}{0.1}\right) = (M_q + M_{\dot{\alpha}})\left(\frac{1}{3} \pm \frac{2}{3}\right) \pm M_{p\beta}(20) \ .$$

From this it can be seen that, on a spin stabilized shell, $M_{p\beta}$ can overwhelm $(M_q + M_{\dot{\alpha}})$ even if it is numerically much smaller; in fact, $M_{p\beta}$ can provide a major part of the damping on a spin stabilized shell. Now if we substitute the numbers for a high fineness ratio fin stabilized rocket with an I_x of 2 and an I of 300 we have

$$\lambda_{1,2} = \left(\frac{M_q + M_{\dot{\alpha}}}{2\,(300)}\right)(1 \pm .01) \pm \frac{M_{p\beta}}{2}(.01)$$

$$\lambda_{1,2} \cong (M_q + M_{\dot{\alpha}})(.0017) \pm M_{p\beta}(.005) \ .$$

Converting the moments to coefficient form,

$$\lambda_{1,2} \cong \left[(C_{mq} + C_{m\dot{\alpha}})(.0017) \pm C_{mp\beta}(.005)\right] qsd \ .$$

Wind tunnel tests have shown a value of 2500/rad for $(C_{mq} + C_{m\dot{\alpha}})$ and 50/rad for $C_{mp\beta}$ on the Nike Tomahawk,[8] a high-fineness-ratio fin-stabilized rocket. While these data indicate that $M_{p\beta}$ has a relatively small effect on the motion of this type of vehicle, one should not make a conclusive judgment on the relative significance of $M_{p\beta}$ in all cases on the basis of a single wind tunnel test.

Conclusions

A highly detailed development of the Tricyclic Theory has been presented and its restrictions discussed. A simplified version of the theory was obtained and two example calculations compared with 6 DOF calculations. This work leads to the following conclusions.

1. Properly applied, the linear Tricyclic Theory provides an excellent means of predicting the motion of rigid bodies.

2. The simplified method of evaluating the K arms will be adequate for many if not most flight dynamics situations.

3. The contribution of the K_3 arm to the magnitude of the K_1 and K_2 arms, which has often been neglected, is significant.

4. The Tricyclic Theory provides a means for understanding flight dynamics problems that are often otherwise incomprehensible.

REFERENCES

1. Nicolaides, J. D., On the Free Flight Motion of Missiles Having Slight Configurational Asymmetries, Ballistic Research Laboratories Report No. 858, June 1953.

2. Nicolaides, J. D., Free Flight Dynamics, Text, Aero-Space Department, University of Notre Dame, Notre Dame, Indiana.

3. Murphy, C. H., Free Flight Motion of Symmetric Missiles, Ballistic Research Laboratories Report No. 1216, July 1963.

4. Scarborough, J. B., The Gyroscope, University Press, Cambridge, 1958.

5. Etkin, Bernard, Dynamics of Flight, John Wiley and Sons, 1962.

6. Halfman, R. L., Dynamics, Addison-Wesley, 1962.

7. Six-Degree-of-Freedom Flight Path Study Generalized Computer Program, FDL-TDR-64-1, Air Force Flight Dynamics Laboratory, Wright-Patterson Air Force Base, Ohio, October 1964.

8. Curry, W. H., and Reed, James F., Measurement of Magnus Effects on a Sounding Rocket Model in a Supersonic Wind Tunnel, AIAA Paper, September 1966.

APPENDIX A

Sample Calculations

Basic Calculations									Tricyclic Example																Epicyclic Example									
(1)	(2)	(3)	(4)	(5)	(6)	(7)	(8)	(9)	(10)	(11)	(12)	(13)	(14)	(15)	(16)	(17)	(18)	(19)	(20)	(21)	(22)	(23)	(24)	(25)	(26)	(27)	(28)	(29)	(30)	(31)	(32)	(33)	(34)
																				Tricyclic Theory		6 DOF								Tricyclic Theory		6 DOF	
t	$\omega_1 t$ Degrees	$\omega_2 t$ Degrees	$\sin\omega_1 t$	$\cos\omega_1 t$	$\sin\omega_2 t$	$\cos\omega_2 t$	$e^{\lambda_1 t}$	$e^{\lambda_2 t}$	$A_1 e^{\lambda_1 t}$	$A_2 e^{\lambda_2 t}$	$A_1 e^{\lambda_1 t}\cos\omega_1 t$	$A_1 e^{\lambda_2 t}\cos\omega_2 t$	$A_1 e^{\lambda_1 t}\sin\omega_1 t$	$A_2 e^{\lambda_2 t}\sin\omega_2 t$	pt Degrees	sin pt	cos pt	A_3 sin pt	A_3 cos pt	$\bar{\alpha}$	$\bar{\beta}$	$\tilde{\alpha}$	$\tilde{\beta}$	$A_1 e^{\lambda_1 t}$	$A_2 e^{\lambda_2 t}$	$A_1 e^{\lambda_1 t}\cos\omega_1 t$	$A_2 e^{\lambda_2 t}\cos\omega_2 t$	$A_1 e^{\lambda_1 t}\sin\omega_1 t$	$A_2 e^{\lambda_2 t}\sin\omega_2 t$	$\bar{\alpha}$	$\bar{\beta}$	$\tilde{\alpha}$	$\tilde{\beta}$
0	0	0	0	+1.000	0	+1.000	1.000	1.000	4.705	5.354	+4.705	+5.354	0	0	0	0	+1.000	0	-0.059	+10.000	0	+10.000	0	4.501	5.499	+4.501	+5.499	0	0	+10.000	0	+10.000	0
0.05	19.9	- 16.3	-0.341	+0.941	+0.281	+0.960	0.997	0.998	4.691	5.343	+4.414	+5.219	-1.600	+1.501	108	-0.951	-0.309	+0.056	+0.018	+ 9.561	-0.043	+ 9.567	-0.044	4.487	5.488	+4.222	+5.268	-1.530	+1.542	+ 9.490	+0.012	+ 9.497	+0.010
0.10	39.8	- 32.7	-0.640	+0.769	+0.541	+0.831	0.992	0.994	4.667	5.322	+3.589	+4.423	-2.986	+2.879	216	+0.587	-0.809	-0.035	+0.048	+ 8.060	-0.142	+ 8.156	-0.166	4.465	5.466	+3.434	+4.542	-2.858	+2.957	+ 7.976	+0.099	+ 8.075	+0.080
0.15	59.7	- 49.0	-0.864	+0.504	+0.755	+0.655	0.987	0.992	4.644	5.311	+2.341	+3.479	-4.012	+4.010	325	+0.573	+0.820	-0.034	-0.049	+ 5.771	-0.036	+ 5.846	-0.064	4.442	5.455	+2.239	+3.573	-3.838	+4.118	+5.812	+0.280	+ 5.886	+0.254
0.20	79.7	- 65.4	-0.984	+0.179	+0.910	+0.416	0.985	0.988	4.634	5.290	+0.829	+2.201	-4.560	+4.814	432	-0.951	-0.309	+0.056	+0.018	+ 3.048	+0.310	+ 3.120	+0.285	4.433	5.433	+0.794	+2.260	-4.362	+4.944	+ 3.054	+0.582	+ 3.162	+0.553
0.25	99.5	- 81.3	-0.986	-0.165	+0.986	+0.151	0.982	0.984	4.620	5.268	-0.762	+0.794	-4.555	+5.215	540	0	-1.000	0	+0.059	+ 0.091	+0.660	+ 0.184	+0.639	4.420	5.411	-0.729	+0.817	-4.358	+5.335	+ 0.088	+0.977	+ 0.179	+0.972
0.30	119.6	- 97.8	-0.869	-0.494	+0.991	-0.136	0.977	0.981	4.598	5.252	-2.271	-0.714	-3.997	+5.205	649	+0.946	+0.326	-0.056	-0.019	- 3.004	+1.152	- 2.857	+1.117	4.397	5.395	-2.172	-0.734	-3.821	+5.346	- 2.906	+1.525	- 2.760	+1.480
0.35	139.3	-113.9	-0.652	-0.758	+0.914	-0.405	0.974	0.977	4.583	5.231	-3.474	-2.119	-2.988	+4.781	757	-0.602	+0.799	+0.036	-0.047	- 5.640	+1.829	- 5.507	+1.806	4.384	5.373	-3.323	-2.176	-2.858	+4.911	- 5.499	+2.053	- 5.369	+2.021
0.40	159.2	-130.1	-0.355	-0.935	+0.765	-0.644	0.970	0.975	4.564	5.220	-4.267	-3.362	-1.620	+3.993	865	-0.574	-0.819	+0.034	+0.049	- 7.580	+2.407	- 7.439	+2.382	4.366	5.362	-4.082	-3.453	-1.550	+4.102	- 7.535	+2.552	- 7.397	+2.516
0.45	179.1	-146.4	-0.016	-1.000	+0.553	-0.833	0.966	0.973	4.545	5.209	-4.545	-4.339	-0.073	+2.776	972	+0.951	-0.309	-0.056	+0.018	- 8.866	+2.647	- 8.716	+2.740	4.348	5.350	-4.348	-4.457	-0.070	+2.959	- 8.805	+2.889	- 8.657	+2.869
0.50	199.0	-162.7	+0.326	-0.946	+0.297	-0.955	0.964	0.969	4.536	5.188	-4.291	-4.955	+1.479	+1.541	1081	-0.017	+1.000	0	-0.059	- 9.305	+3.020	- 9.154	+3.020	4.339	5.329	-4.105	-5.089	+1.415	+1.583	- 9.194	+2.998	- 9.047	+2.988
0.55	218.9	-178.9	+0.628	-0.778	+0.019	-1.000	0.958	0.966	4.507	5.172	-3.506	-5.172	+2.830	+0.098	1189	-0.946	-0.326	+0.056	+0.019	- 8.659	+2.984	- 8.545	+2.990	4.312	5.312	-3.355	-5.312	+2.708	+0.101	- 8.667	+2.809	- 8.554	+2.803
0.60	238.8	-195.2	+0.855	-0.518	-0.262	-0.965	0.955	0.963	4.493	5.156	-2.327	-4.976	+3.788	-1.351	1297	+0.602	-0.799	-0.036	+0.047	- 7.256	+2.401	- 7.171	+2.461	4.298	5.296	-2.226	-5.111	+3.675	-1.388	- 7.337	+2.287	- 7.254	+2.288
0.65	258.7	-211.4	+0.981	-0.193	-0.521	-0.854	0.952	0.960	4.478	5.140	-0.864	-4.389	+4.393	-2.678	1405	+0.574	+0.819	-0.034	-0.049	- 5.302	+1.681	- 5.270	+1.690	4.285	5.279	-0.827	-4.508	+4.204	-2.750	- 5.335	+1.454	- 5.302	+1.460
0.70	278.6	-227.7	+0.989	+0.150	-0.739	-0.673	0.948	0.957	4.460	5.124	+0.669	-3.448	+4.411	-3.787	1514	-0.951	+0.309	+0.056	-0.018	- 2.797	+0.680	- 2.811	+0.722	4.267	5.263	+0.640	-3.542	+4.220	-3.889	- 2.902	+0.331	- 2.912	+0.376
0.75	298.5	-244.0	+0.879	+0.447	-0.899	-0.438	0.945	0.954	4.446	5.108	+2.121	-2.237	+3.908	-4.592	1621	0	-1.000	0	+0.059	- 0.057	-0.680	- 0.130	-0.594	4.253	5.246	+2.029	-2.298	+3.738	-4.716	- 0.269	-0.978	- 0.336	-0.878
0.80	318.4	-260.2	+0.664	+0.748	-0.985	-0.170	0.940	0.951	4.423	5.092	+3.308	-0.865	+2.937	-5.016	1730	+0.946	+0.326	-0.056	-0.019	+ 2.424	-2.135	+ 2.305	-1.999	4.231	5.230	+3.165	-0.889	+2.809	-5.152	+ 2.276	-2.343	- 2.165	-2.194
0.85	338.3	-276.5	+0.370	+0.929	-0.994	+0.113	0.937	0.948	4.409	5.076	+4.096	+0.574	+1.631	-5.046	1838	-0.602	+0.799	+0.036	-0.047	+ 4.623	-3.379	+ 4.454	-3.213	4.217	5.213	+3.918	+0.589	+1.560	-5.182	+ 4.507	-3.622	- 4.349	-3.441
0.90	358.2	-292.8	+0.031	+1.000	-0.922	+0.388	0.933	0.945	4.390	5.060	+4.390	+1.963	+0.136	-4.665	1946	-0.574	-0.819	+0.034	+0.049	+ 6.375	-4.495	+ 6.191	-4.324	4.199	5.197	+4.199	+2.009	+0.130	-4.792	+ 6.208	-4.662	- 6.107	-4.475
0.95	378.1	-309.0	-0.311	+0.951	-0.777	+0.629	0.930	0.942	4.376	5.044	+4.162	+3.173	-1.361	-3.919	2053	+0.951	-0.309	-0.056	+0.018	+ 7.353	-5.336	+ 7.130	-5.177	4.186	5.180	+3.981	+3.258	-1.302	-4.025	+ 7.239	-5.327	- 7.030	-5.150
1.00	398.0	-325.3	-0.616	+0.788	-0.569	+0.822	0.927	0.939	4.362	5.027	+3.437	+4.132	-2.687	-2.860	2160	-0.017	+1.000	0	-0.059	+ 7.510	-5.547	+ 7.292	-5.403	4.172	5.164	+2.288	+4.245	-2.570	-2.938	+ 7.533	-5.508	- 7.324	-5.351
1.05	417.9	-341.6	-0.847	+0.531	-0.316	+0.949	0.923	0.936	4.343	5.011	+2.306	+4.755	-3.679	-1.583	2270	-0.946	-0.326	+0.056	+0.019	+ 7.080	-5.206	+ 6.892	-5.084	4.154	5.147	+2.206	+4.885	-3.518	-1.626	+ 7.091	-5.144	- 6.910	-5.125
1.10	437.8	-357.8	-0.977	+0.211	-0.038	+0.999	0.920	0.933	4.329	4.995	+0.913	+4.990	-4.229	-0.190	2377	+0.602	-0.799	-0.036	+0.047	+ 5.950	-4.455	+ 5.814	-4.358	4.141	5.131	+0.874	+5.126	-4.046	-0.195	+ 6.000	-4.241	- 5.866	-4.139

DISTRIBUTION:
Standard Aero-Thermo Dynamics Distribution List (195)
STA Membership and Military (100)
W. J. Howard, 1000
C. F. Bild, 1100
L. A. Hopkins, 1300
R. E. Fox, 1325
J. H. Findlay, 1400
W. A. Gardner, 1500
T. B. Lane, 1540
R. T. Othmer, 1541
F. J. Perdreauville, 1541
T. B. Cook, 5000
R. S. Claassen, 5100
J. W. Weihe, 5250
M. J. Norris, 5260
L. D. Smith, 5500
R. L. Peurifoy, 5510
A. A. Lieber, 5540
D. B. Shuster, 5600
G. W. Rodgers, 5620
R. G. Clem, 5630
L. E. Hollingsworth, 7200
T. L. Pace, 7210
L. Gutierrez, 8100
A. N. Blackwell, 8110
G. W. Anderson, 8140
A. R. Willis, 8147
G. A. Fowler, 9000
J. H. Scott, 9200
J. C. Eckhart, 9220
A. Y. Pope, 9300
V. E. Blake, 9310
S. McAlees, 9314
G. W. Stone, 9314 (25)
R. C. Maydew, 9320
H. R. Vaughn, 9321 (125)
W. H. Curry, 9322
E. C. Rightley, 9323
W. R. Barton, 9324
J. K. Cole, 9325
K. J. Touryan, 9326
W. N. Caudle, 9327
D. F. McVey, 9328
A. J. Clark, 9330
W. C. Scrivner, 9400
J. A. Allensworth, 9422
B. R. Allen, 3421
L. C. Baldwin, 3412
B. F. Hefley, 8232
R. S. Gillespie, 3413
For: DTIE (3)
For: H. F. Carroll (1)
W. H. Swiss, 3413
C. H. Sproul, 3428-2 (10)

SECOND PRINTING:
C. H. Sproul, 3428-2 (50)
A. R. Willis, 8313 (50)
H. R. Vaughn, 9325 (100)